Arch Computat Methods Eng (2017) 24:495–518
DOI 10.1007/s11831-016-9178-z

ORIGINAL PAPER

A Critical Assessment of Kriging Model Variants for High-Fidelity Uncertainty Quantification in Dynamics of composite Shells

T. Mukhopadhyay[1] · S. Chakraborty[2] · S. Dey[3] · S. Adhikari[1] · R. Chowdhury[2]

Received: 2 March 2016 / Accepted: 5 April 2016 / Published online: 13 April 2016

Abstract This paper presents a critical comparative assessment of Kriging model variants for surrogate based uncertainty propagation considering stochastic natural frequencies of composite doubly curved shells. The five Kriging model variants studied here are: Ordinary Kriging, Universal Kriging based on pseudo-likelihood estimator, Blind Kriging, Co-Kriging and Universal Kriging based on marginal likelihood estimator. First three stochastic natural frequencies of the composite shell are analysed by using a finite element model that includes the effects of transverse shear deformation based on Mindlin's theory in conjunction with a layer-wise random variable approach. The comparative assessment is carried out to address the accuracy and computational efficiency of five Kriging model variants. Comparative performance of different covariance functions is also studied. Subsequently the effect of noise in uncertainty propagation is addressed by using the Stochastic Kriging. Representative results are presented for both individual and combined stochasticity in layer-wise input parameters to address performance of various Kriging variants for low dimensional and relatively higher dimensional input parameter spaces. The error estimation and convergence studies are conducted with respect to original Monte Carlo Simulation to justify merit of the present investigation. The study reveals that Universal Kriging coupled with marginal likelihood estimate yields the most accurate results, followed by Co-Kriging and Blind Kriging. As far as computational efficiency of the Kriging models is concerned, it is observed that for high-dimensional problems, CPU time required for building the Co-Kriging model is significantly less as compared to other Kriging variants.

✉ T. Mukhopadhyay
mukhopadhyay.mail@gmail.com; 800712@swansea.ac.uk;
http://www.tmukhopadhyay.com

S. Chakraborty
chin2dce@iitr.ac.in

[1] College of Engineering, Swansea University, Swansea, UK

[2] Department of Civil Engineering, Indian Institute of Technology Roorkee, Roorkee, India

[3] Leibniz-Institut für Polymerforschung Dresden e.V., Dresden, Germany

1 Introduction

The inherent problem of computational modelling dealing with empirical data is germane to many engineering applications particularly when both input and output quantities are uncertain in nature. In empirical data modeling, a process of induction is employed to build up a model of the system from which it is assumed to deduce the responses of the system that have yet to be observed. Ultimately both quantity and quality of the observations govern the performance of the empirical model. By its observational nature, data obtained is finite and sampled; typically when this sampling is non-uniform and due to high dimensional nature of the problem, the data will form only a sparse distribution in the input space.

Due to inherent complexity of composite materials, such variability of output with respect to randomness in input parameters is difficult to map computationally by means of deterministic finite element models. In general, composite materials are extensively employed in aerospace, automotive, construction, marine and many other industries for its high specific stiffness and strength with added advantages of weight sensitivity (refer Fig. 1). For example, about 25 and 50 % of their total weight is made of composites in

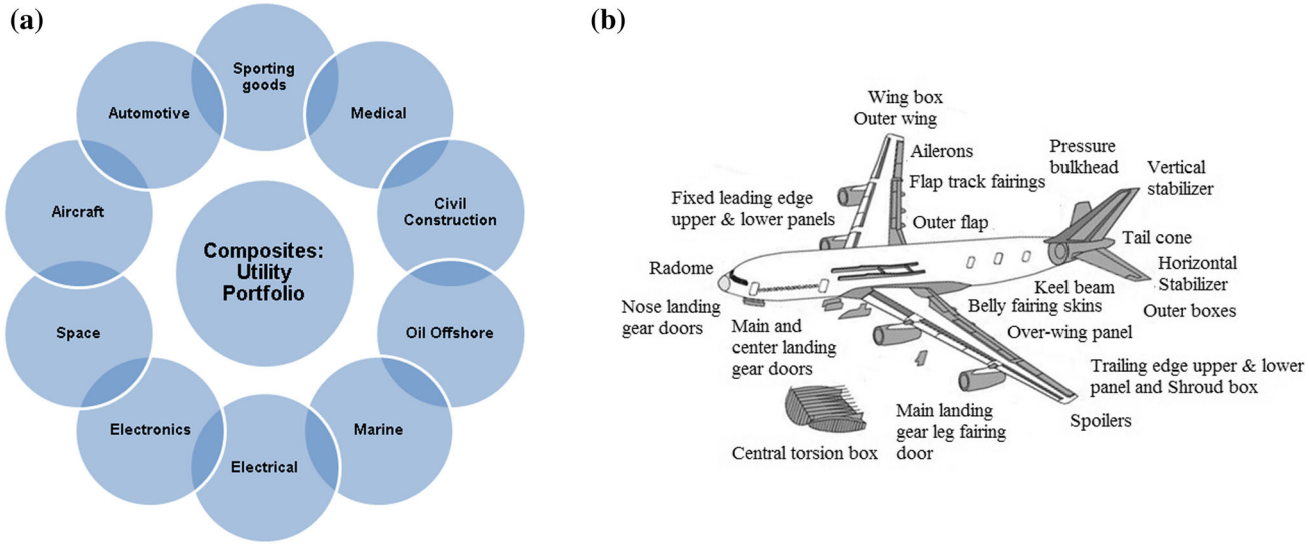

Fig. 1 **a** Application of FRP composites across various engineering fields. **b** Structural components made of composites in Airbus A380

modern aircrafts such as Airbus A380 and Boeing 787 respectively [1]. Due to the intricacies involved in production process, laminated composite shells are difficult to manufacture accurately according to its exact design specifications which in turn can affect the dynamic characteristics of its components [1, 2]. It involves many sources of uncertainty associated with variability in geometric properties, material properties and boundary conditions. The uncertainty in any sensitive input parameter may propagate to influence the other parameters of the system leading to unknown trends of output behavior. In general, the fibre and matrix are fabricated with three basic steps namely tape, layup and curing. The properties of constituent material vary randomly due to lack of accuracy that can be maintained with respect to its exact designed properties in each layer of the laminate. The intra-laminate voids or porosity, excess matrix voids or excess resin between plies, incomplete curing of resin and misalignment of ply-orientation are caused by natural inaccuracies due to man, machine and method of operation. These are the common root-causes of uncertainties incurred during the production process. Moreover any damage or defects incurred due to such variability and during operation period (such as environmental factors like temperature and moisture, rotational uncertainty etc.) of the structures can compromise the performance of composite components, which in turn lead to the use of more conservative designs that do not fully exploit the performance and behavior of such structures. As a consequence, the dynamic responses of composite structures show considerable fluctuation from its mean deterministic value. Due to complexity involved in ascertaining the stochastic bandwidth of output quantities, designers generally bridge these gaps by introducing a concept of over design; the term being popularly known as factor of safety. The consideration of such additional factor of safety due to uncertainty may lead to result in either an unsafe design or an ultraconservative and uneconomic design. In view of the above, it is needless to mention that the structural stability and intended performance of any engineering system are always governed by considerable element of inherent uncertainty. Sometimes the interaction trends of input quantities are not sufficient to map the domain of uncertainty precisely. The cascading effect of such unknown trend creates the deviation from expected zone of uncertainty. Therefore, it is mandatory to estimate the variability in output quantities such as natural frequencies linked with the expected performance characteristic to ensure the operational safety. The critical assessment of uncertain natural frequency of composite structures has gained wide spectrum of demand in engineering applications. However, the common modes of uncertainty quantification in composites are usually computationally quite expensive. Different surrogate based approaches to alleviate the computational cost of uncertainty propagation has become a popular topic of research in last couple of years. Brief description about the lacuna of traditional Monte Carlo simulation (MCS) based uncertainty quantification and application of surrogates in this field are provided in the preceding paragraphs.

In general, uncertainty can be broadly categorized into three classes namely, aleatoric (due to variability in the system parameters), epistemic (due to lack of knowledge of the system) and prejudicial (due to absence of variability characterization). The well-known MCS technique [3, 4] is employed universally to characterize the stochastic output parameter considering large sample size and thus, thousands of model evaluations (finite element simulations) are generally needed. Therefore, traditional MCS based

uncertainty quantification approach is inefficient for practical purposes and incurs high computational cost. To avoid such lacuna, present investigation includes the Kriging model as surrogate for reducing the computational time and cost in mapping the uncertain natural frequencies. In this approach of uncertainty quantification, the computationally expensive finite element model is effectively replaced by an efficient mathematical model and thereby, thousands of virtual simulations can be carried out in a cost-effective manner. A concise review on Kriging models and their applications are given in the next paragraph.

Significant volume of scientific studies is found to be reported on Kriging model and its applications in various engineering problems [4–11]. Further studies on the basis of design and analysis of experiments are also carried out [12–14]. Several literatures are also found to address different problems related to in optimization [15, 16] and geostatistics [17] using Kriging model. Many researchers proposed a lot of improved methods to solve the problems with computational efficiency based on sampling. Importance Sampling [18–20] is the generic method to achieve comparatively better sampling efficiency and ease of implementation wherein equal attention is provided in both low and high density zone of sample points. In contrast, the important sampling increases the simulation efficiency to a certain extent, but the number of effective samples required to map the actual performance is still excessive. Few studies have concentrated on different variants of Kriging model [20–26] such as Universal Kriging, Co-Kriging, Stochastic Kriging dealing with various engineering problems. Kersaudy et al. [27] have studied a new surrogate modelling technique combining Kriging and polynomial chaos expansions for uncertainty analysis. Khodaparast et al. [28] have used interval model updating with irreducible uncertainty using the Kriging predictor. Sensitivity analysis based on Kriging models for robust stability of brake systems has been conducted by Nechak et al. [29]. Pigoli et al. [30] have studied manifold-valued random fields by Kriging model. The uncertainty quantification in DIC with Kriging regression is found to be studied by Wang et al. [31]. A range of Kriging based investigations have been reported for different field of applications with probabilistic approach [32–36]. The Co-Kriging is employed recently for dealing with optimization of the cyclone separator geometry for minimum pressure drop [37]. An improved moving Kriging-based mesh-free method is employed for static, dynamic and buckling analyses of functionally graded isotropic and sandwich plates by Thai et al. [38]. Kriging is found to be employed for reliability analysis by Yang et al. [39] and Gaspar et al. [40]. Huang et al. [41] have investigated assessment of small failure probabilities by combining Kriging and Subset Simulation. Kwon et al. [42] have studied to find the trended Kriging model with R^2 indicator and application to design optimization. Apart from the application of Kriging models encompassing different domains of engineering in general as discussed above, few recent applications of Kriging model in the field of composites can be found. Sakata et al. have studied on Kriging-based approximate stochastic homogenization analysis for composite materials [43]. Luersen et al. [44] have carried out Kriging based optimization for path of curve fiber in composite laminates. In the next paragraph, as per the focus of this article, we concentrate on free vibration analysis of laminated composites following both deterministic and stochastic paradigm.

The deterministic approach for bending, buckling and free vibration analysis of composite plates and shells are exhaustively investigated by many researchers in past [45–55]. Recently the topic of quantifying uncertainty for various static and dynamic responses of composite structures has gained attention from the concerned research community [56–67]. Early researches concentrated on design of composite laminates using direct MCS [56] and progressive failure models in a probabilistic framework [57]. Over the last decade several studies have been reported to quantify uncertainty in bending, buckling and failure analysis of composites with the consideration of micro and macro-mechanical material properties including sandwich structures [58–67]. However, the aspect of stochastic free vibration characteristics of composite plate and curved shells has not received adequate attention [68–73]. Most of the studies concerning laminated composites as cited above are based on parametric uncertainties with random material and geometric properties. Perturbation based method and MCS method are the two predominant approaches followed in this studies. Recently surrogate based stochastic analysis for laminated composite plates have started gaining attention from the research community due to computational convenience [69, 71]. Comparative study of different surrogate models are essential from practical design perspective to provide an idea about which surrogate is best suitable for a particular problem. Though the open literature confirms that the Kriging provides a rational means for creating experimental designs for surrogate modeling as discussed in the previous paragraph, application of different Kriging variants in stochastic natural frequency analysis of composite laminates is scarce to find in scientific literature. Moreover, assessment of the comparative performance of different Kriging variants on the basis of accuracy and computational efficiency is very crucial.

To fill up the above mentioned apparent void, the present analyses employs finite-element approach to study the stochastic free vibration characteristics of graphite–epoxy composite cantilever shallow curved shells by using

five different Kriging surrogate model variants namely, Ordinary Kriging, Universal Kriging based on pseudo-likelihood estimator, Blind Kriging, Co-Kriging and Universal Kriging based on marginal likelihood estimator. The finite element formulation considering layer-wise random system parameters in a non-intrusive manner is based on consideration of eight noded isoparametric quadratic element with five degrees of freedom at each node. The selective representative samples for construction Kriging models are drawn using Latin hypercube sampling algorithm [74] over the entire domain ensuring good prediction capability of the constructed surrogate model. The distinctive comparative studies on efficiencies of aforesaid five Kriging model variants have been carried out in this study to assess their individual merits on the basis of accuracy and computational efficiency. Both individual and combined stochasticity in input parameters such as ply orientation angle, elastic modulus, mass density, shear modulus and Poisson's ratio have been considered for this computational investigation. The precision and accuracy of results obtained from the constructed surrogate models have been verified with respect to original finite element simulation. To the best of the authors' knowledge, there is no literature available which deals with comparative computational investigation with the five Kriging model variants for uncertainty quantification of natural frequency of composite curved shells considering both low and high dimensional input parameter space. Hereafter this article is organized as, Sect. 2: finite element formulation for laminated composite curved shells considering layer-wise stochastic input parameters; Sect. 3: formulation of the five Kriging model variants; Sect. 4: stochastic approach for uncertain natural frequency characterization using finite element analysis in conjunction with the Kriging model variants; Sect. 5: results on comparative assessments considering different crucial aspects and discussion; and Sect. 6: conclusion.

2 Governing Equations for Composite Shell

In present study, a composite cantilever shallow doubly curved shells with uniform thickness 't' and principal radii of curvature R_x and R_y along x- and y-direction respectively is considered as furnished in Fig. 2. Based on the first-order shear deformation theory, the displacement field of the shells may be described as

$$\begin{aligned} \boldsymbol{u}(\boldsymbol{x},\boldsymbol{y},\boldsymbol{z}) &= \boldsymbol{u}^0(\boldsymbol{x},\boldsymbol{y}) - \boldsymbol{z}\theta_x(\boldsymbol{x},\boldsymbol{y}) \\ \boldsymbol{v}(\boldsymbol{x},\boldsymbol{y},\boldsymbol{z}) &= \boldsymbol{v}^0(\boldsymbol{x},\boldsymbol{y}) - \boldsymbol{z}\theta_y(\boldsymbol{x},\boldsymbol{y}) \\ \boldsymbol{w}(\boldsymbol{x},\boldsymbol{y},\boldsymbol{z}) &= \boldsymbol{w}^0(\boldsymbol{x},\boldsymbol{y}) = \boldsymbol{w}(\boldsymbol{x},\boldsymbol{y}) \end{aligned} \tag{1}$$

where u^0, v^0, and w^0 are displacements of the reference plane and θ_x and θ_y are rotations of the cross section relative to x and y axes, respectively. Each of the thin fibre of laminae can be oriented at an arbitrary angle 'θ' with reference to the x-axis. The constitutive equations [47] for the shell are given by

$$\{\boldsymbol{F}\} = [\mathbf{D}(\bar{\omega})]\{\varepsilon\} \tag{2}$$

where

Force resultant $\{F\} = \{N_x, N_y, N_{xy}, M_x, M_y, M_{xy}, Q_x, Q_y\}^T$

$$\{F\} = \left[\int_{-h/2}^{h/2} \{\sigma_x\ \sigma_y\ \tau_{xy}\ \sigma_{xz}\ \sigma_{yz}, \tau_{xyz}\ \tau_{xz}\ \tau_{yz}\} dz\right]^T$$

and strain $\{\varepsilon\} = \{\varepsilon_x, \varepsilon_y, \varepsilon_{xy}, k_x, k_y, k_{xy}, \gamma_{xz}, \gamma_{yz}\}^T$

$$[\boldsymbol{D}(\bar{\omega})] = \begin{bmatrix} \boldsymbol{A}_{16} & \boldsymbol{A}_{26} & \boldsymbol{A}_{66} & \boldsymbol{B}_{16} & \boldsymbol{B}_{26} & \boldsymbol{B}_{66} & 0 & 0 \\ \boldsymbol{B}_{11} & \boldsymbol{B}_{12} & \boldsymbol{B}_{16} & \boldsymbol{D}_{11} & \boldsymbol{D}_{12} & \boldsymbol{D}_{16} & 0 & 0 \\ \boldsymbol{B}_{12} & \boldsymbol{B}_{22} & \boldsymbol{B}_{26} & \boldsymbol{D}_{12} & \boldsymbol{D}_{22} & \boldsymbol{D}_{26} & 0 & 0 \\ \boldsymbol{B}_{16} & B_{26} & \boldsymbol{B}_{66} & \boldsymbol{D}_{16} & \boldsymbol{D}_{26} & \boldsymbol{D}_{66} & 0 & 0 \\ 0 & 0 & 0 & 0 & 0 & 0 & \boldsymbol{S}_{44} & \boldsymbol{S}_{45} \\ 0 & 0 & 0 & 0 & 0 & 0 & \boldsymbol{S}_{45} & \boldsymbol{S}_{55} \end{bmatrix}$$

The elements of elastic stiffness matrix $[D(\bar{\omega})]$ can be expressed as

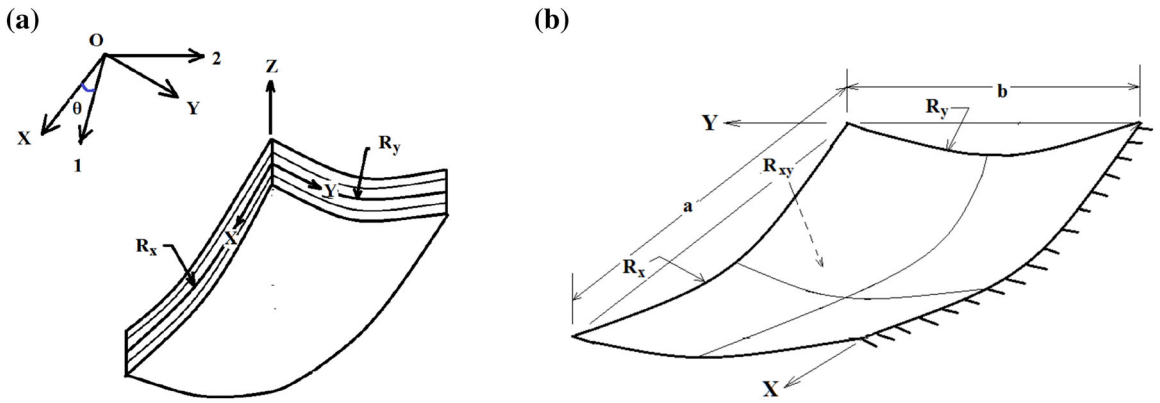

Fig. 2 Laminated composite shallow doubly curved shell model

$$[A_{ij}(\bar{\omega}), B_{ij}(\bar{\omega}), D_{ij}(\bar{\omega})] = \sum_{k=1}^{n} \int_{z_{k-1}}^{z_k} [\{\bar{Q}_{ij}(\bar{\omega})\}_{on}]_k [1, z, z^2] dz$$
$$i,j = 1,2,6 \tag{3}$$

where $\bar{\omega}$ indicates the stochastic representation and α_s is the shear correction factor (=5/6) and $[\bar{Q}_{ij}]$ are elements of the off-axis elastic constant matrix which is given by

$$[\bar{Q}_{ij}]_{off} = [T_1(\bar{\omega})]^{-1} [\bar{Q}_{ij}]_{on} [T_1(\bar{\omega})]^{-T} \quad \text{for} \quad i,j = 1,2,6$$
$$[\bar{Q}_{ij}]_{off} = [T_2(\bar{\omega})]^{-1} [\bar{Q}_{ij}]_{on} [T_2(\bar{\omega})]^{-T} \quad \text{for} \quad i,j = 4,5 \tag{4}$$

and

$$[T_1(\bar{\omega})] = \begin{bmatrix} m^2 & n^2 & 2mn \\ n^2 & m^2 & -2mn \\ -mn & mn & m^2 \end{bmatrix} \quad \text{and}$$
$$[T_2(\bar{\omega})] = \begin{bmatrix} m & -n \\ n & m \end{bmatrix} \tag{5}$$

in which $m = \text{Sin}\theta(\bar{\omega})$ and $n = \text{Cos}\theta(\bar{\omega})$, wherein $\theta(\bar{\omega})$ is random fibre orientation angle.

$$\left[Q_{ij}(\bar{\omega})\right]_{on} \begin{bmatrix} Q_{11} & Q_{12} & 0 \\ Q_{12} & Q_{12} & 0 \\ 0 & 0 & Q_6 \end{bmatrix} \quad \text{for}$$
$$\text{i, j = 1,2,6} \left[\bar{Q}_{ij}(\bar{\omega})\right]_{on} = \begin{bmatrix} Q_{44} & Q_{45} \\ Q_{45} & Q_{55} \end{bmatrix} \quad \text{for} \quad \text{i = 4,5} \tag{6}$$

where

$$Q_{11} = \frac{E_1}{1 - v_{12}v_{21}} \; Q_{22} = \frac{E_2}{1 - v_{12}v_{21}} \text{ and } Q_{12} = \frac{v_{12}E_2}{1 - v_{12}v_{21}}$$
$$Q_{66} = G_{12} \; Q_{44} = G_{23} \text{ and } Q_{55} = G_{13}$$

.

The strain–displacement relations for shallow doubly curved shells can be expressed as

$$\begin{Bmatrix} \varepsilon_x \\ \varepsilon_y \\ \gamma_{xy} \\ \gamma_{xz} \\ \gamma_{yz} \end{Bmatrix} = \begin{Bmatrix} \frac{\partial u}{\partial x} - \frac{w}{R_x} \\ \frac{\partial v}{\partial y} - \frac{w}{R_y} \\ \frac{\partial u}{\partial y} + \frac{\partial v}{\partial x} - \frac{2w}{R_{xy}} \\ \theta_x + \frac{\partial w}{\partial x} \\ \theta_y + \frac{\partial w}{\partial y} \end{Bmatrix}, \begin{Bmatrix} k_x \\ k_y \\ k_{xy} \\ k_{xz} \\ k_{yz} \end{Bmatrix} = \begin{Bmatrix} \frac{\partial \theta_x}{\partial x} \\ \frac{\partial \theta_y}{\partial y} \\ \frac{\partial \theta_x}{\partial y} + \frac{\partial \theta_y}{\partial x} \\ 0 \\ 0 \end{Bmatrix}$$
$$\text{and } \{\varepsilon\} = [B]\{\delta_e\}$$
$$\{\delta_e\} = \{u_1, v_1, w_1, \theta_{x1}, \theta_{y1}, \ldots u_8, v_8, w_8, \theta_{x8}, \theta_{y8}\}^T \tag{7}$$

where

$$[B] = \sum_{i=1}^{8} \begin{bmatrix} N_{i,x} & 0 & -\frac{N_i}{R_x} & 0 & 0 \\ 0 & N_{i,y} & -\frac{N_i}{R_y} & 0 & 0 \\ N_{i,y} & N_{i,x} & -\frac{2N_i}{R_{xy}} & 0 & 0 \\ 0 & 0 & 0 & N_{i,x} & 0 \\ 0 & 0 & 0 & 0 & N_{i,y} \\ 0 & 0 & 0 & N_{i,y} & N_{i,x} \\ 0 & 0 & N_{i,x} & N_i & 0 \\ 0 & 0 & N_{i,y} & 0 & N_i \end{bmatrix}$$

where R_{xy} is the radius of curvature in xy-plane of shallow doubly curved shells and $k_x, k_y, k_{xy}, k_{xz}, k_{yz}$ are curvatures of the shell and u, v, w are the displacements of the mid-plane along x, y and z axes, respectively. An eight noded isoparametric quadratic element with five degrees of freedom at each node (three translations and two rotations) is considered wherein the shape functions (N_i) are as follows [75]

$$N_i = \frac{(1 + \chi\chi_i)(1 + \varsigma\varsigma_i)(\chi\chi_i + \varsigma\varsigma_i - 1)}{4} \quad (\text{for } i = 1,2,3,4) \tag{8}$$

$$N_i = \frac{(1 - \chi^2)(1 + \varsigma\varsigma_i)}{2} \quad (\text{for } i = 5,7) \tag{9}$$

$$N_i = \frac{(1 - \varsigma^2)(1 + \chi\chi_i)}{2} \quad (\text{for } i = 6,8) \tag{10}$$

where ς and χ are the local natural coordinates of the element. The mass per unit area for curved shell can be expressed as

$$P(\bar{\omega}) = \sum_{k=1}^{n} \int_{z_{k-1}}^{z_k} \rho(\bar{\omega})\, dz \tag{11}$$

where $\rho(\bar{\omega})$ is the random mass density of the laminate. The mass matrix can be expressed as

$$[M(\bar{\omega})] = \int_{Vol} [N][P(\bar{\omega})][N] d(vol) \tag{12}$$

where

$$[N] = \begin{bmatrix} N_i & & & & \\ & N_i & & & \\ & & N_i & & \\ & & & N_i & \\ & & & & N_i \end{bmatrix} \quad \text{and}$$
$$[P(\bar{\omega})] = \begin{bmatrix} P(\bar{\omega}) & 0 & 0 & 0 & 0 \\ & P(\bar{\omega}) & 0 & 0 & 0 \\ & & P(\bar{\omega}) & 0 & 0 \\ & & & I(\bar{\omega}) & 0 \\ Sym & & & & I(\bar{\omega}) \end{bmatrix}$$

Here the fourth and fifth diagonal element i.e., $I(\bar{\omega})$ depicts the random rotary inertia. The stiffness matrix is given by

$$[K(\bar{\omega})] = \int_{-1}^{1}\int_{-1}^{1} [B(\bar{\omega})]^T [D(\bar{\omega})]\,[B(\bar{\omega})] d\varsigma\, d\chi \tag{13}$$

The Hamilton's principle [76] is employed to study the dynamic nature of the composite structure. The principle used for the Lagrangian which is defined as

$$L_f = T - U - W \tag{14}$$

where T, U and W are total kinetic energy, total strain energy and total potential of the applied load, respectively. The Hamilton's principle applicable to non-conservative system is expressed as,

$$\delta H = \int_{p_i}^{p_f} [\delta T - \delta U - \delta W] dp = 0 \tag{15}$$

Hamilton's principle applied to dynamic analysis of elastic bodies states that among all admissible displacements which satisfy the specific boundary conditions, the actual solution makes the functional $\int (T + V) dp$ stationary, where T and W are the kinetic energy and the work done by conservative and non-conservative forces, respectively. For free vibration analysis (i.e., $\delta W = 0$), the stationary value is actually a minimum. In case of a dynamic problem without damping the conservative forces are the elastic forces developed within a deformed body and the non-conservative forces are the external force functions. The energy functional for Hamilton's principle is the Lagrangian (L_f) which includes kinetic energy (T) in addition to potential strain energy (U) of an elastic body. The expression for kinetic energy of an element is expressed as

$$T = \frac{1}{2}\{\dot{\delta}_e\}^T [M_e(\bar{\omega})]\{\dot{\delta}_e\} \tag{16}$$

The potential strain energy for an element of a plate can be expressed as,

$$\begin{aligned} U &= U_1 + U_2 \\ &= \frac{1}{2}\{\delta_e\}^T [K_e(\bar{\omega})]\{\delta_e\} + \frac{1}{2}\{\delta_e\}^T [K_{\sigma e}(\bar{\omega})]\{\delta_e\} \end{aligned} \tag{17}$$

The Langrange's equation of motion is given by

$$\frac{d}{dt}\left[\frac{\partial L_f}{\partial \dot{\delta}_e}\right] - \left[\frac{\partial L_f}{\partial \delta_e}\right] = \{F_e\} \tag{18}$$

where $\{F_e\}$ is the applied external element force vector of an element and L_f is the Lagrangian function. Substituting $L_f = T - U$, and the corresponding expressions for T and U in Lagrange's equation, the dynamic equilibrium equation for each element expressed as [48]

$$[M(\bar{\omega})]\left\{\ddot{\delta}_e\right\} + ([K_e(\bar{\omega})] + K_{\sigma e}(\bar{\omega}))\{\delta_e\} = \{F_e\} \tag{19}$$

After assembling all the element matrices and the force vectors with respect to the common global coordinates, the equation of motion of a system with n degrees of freedom can expressed as

$$[M(\bar{\omega})][\ddot{\delta}] + [K(\bar{\omega})]\{\delta\} = \{F_L\} \tag{20}$$

In the above equation, $M(\bar{\omega}) \in R^{n\times n}$ is the mass matrix, $[K(\bar{\omega})]$ is the stiffness matrix wherein $[K(\bar{\omega})] = [K_e(\bar{\omega})] + [K_{\sigma e}(\bar{\omega})]$ in which $K_e(\bar{\omega}) \in R^{n\times n}$ is the elastic stiffness matrix, $K_{\sigma e}(\bar{\omega}) \in R^{n\times n}$ is the geometric stiffness matrix (depends on initial stress distribution) while $\{\delta\} \in R^n$ is the vector of generalized coordinates and $\{F_L\} \in R^n$ is the force vector. For free vibration analysis the force vector becomes zero. The governing equations are derived based on Mindlin's theory incorporating rotary inertia, transverse shear deformation. For free vibration, the random natural frequencies $[\omega_n(\bar{\omega})]$ are determined from the standard eigenvalue problem [74] which is solved by the QR iteration algorithm.

$$[A(\bar{\omega})]\{\delta\} = \lambda(\bar{\omega})\{\delta\} \tag{21}$$

where

$$[A(\bar{\omega})] = [K(\bar{\omega})]^{-1}[M(\bar{\omega})]$$

$$\lambda(\bar{\omega}) = \frac{1}{\{\omega_n(\bar{\omega})\}^2}$$

3 Kriging Models

In general, a surrogate is an approximation of the Input/Output (I/O) function that is implied by the underlying simulation model. Surrogate models are fitted to the I/O data produced by the experiment with the simulation model. This simulation model may be either deterministic or random (stochastic). The Kriging model was initially developed in spatial statistics by Krige [77] and subsequently extended by Matheron [2] and Cressie [3]. Kriging is a Gaussian process based modelling method, which is compact and cost effective for computation. The basic idea of this method is to incorporate interpolation, governed by prior covariances, to obtain the responses at the unknown points. However as pointed out by various researchers [78–81], results obtained using ordinary Kriging are often erroneous, specifically for problems that are highly nonlinear in nature. In order to address this issue, the universal Kriging has been proposed in [82–86]. In this method, the unknown response is represented as:

$$\boldsymbol{y}(\boldsymbol{x}) = \boldsymbol{y}_0(\boldsymbol{x}) + \boldsymbol{Z}(\boldsymbol{x}) \tag{22}$$

where $y(x)$ is the unknown function of interest, x is an m dimensional vector (m design variables), $y_0(x)$ is the known approximation (usually polynomial) function and $Z(x)$ represents is the realization of a stochastic process with mean zero, variance, and nonzero covariance. In the model, the local deviation at an unknown point (x) is expressed using stochastic processes. The sample points are interpolated with the Gaussian random function as the correlation function to estimate the trend of the stochastic processes. The $y_0(x)$ term is similar to a polynomial response surface, providing global model of the design space [43]. However, the maximum order of the polynomial $y_0(x)$ is often randomly chosen in universal Kriging. This often renders the universal Kriging inefficient and erroneous In order to address the issue associated with universal Kriging, blind Kriging has been proposed in [87–89]. In this method, the polynomial $y_0(x)$ is selected in an adaptive manner. As a consequence, blind Kriging is highly robust. Other variants of Kriging surrogate includes Co-Kriging [90–93] and stochastic Kriging [94–100]. While Co-Kriging yields multi-fidelity results, stochastic Kriging incorporates the noise present in experimental data. Next brief description of various Kriging variants has been provided.

3.1 Ordinary Kriging

In ordinary Kriging, one seeks to predict the value of a function at a given point by computing a weighted average of the known values of the function in the neighbourhood of the point. Kriging is formulated by (1) assuming some suitable covariances, (2) utilizing the Gauss-Markov theorem to prove the independence of the estimate and the error. Provided suitable covariance function is selected, kriging yields the best unbiased linear estimate.

Remark 1 Simple Kriging is a variant of the ordinary Kriging. While in simple Kriging, $y_0(x) = 0$ is assumed, the ordinary Kriging assumes $y_0(x) = a_0$, where α_0 is unknown constant.

3.2 Universal Kriging

A more generalised version of the ordinary Kriging is the universal Kriging. Here, $y_0(x)$ is represented by using a multivariate polynomial as:

$$y_0(x) = \sum_{i=1}^{p} a_i b_i(\mathrm{x}) \tag{23}$$

where $b_i(\mathrm{x})$ represents the ith basis function and a_i denotes the coefficient associated with the ith basis function. The primary idea behind such a representation is that the regression function captures the Largent variance in the data (the overall trend) and the Gaussian process interpolates the residuals. Suppose $X = \{x^1, x^2, \ldots, x^n\}$ represents a set of n samples. Also assume $Y = \{y_1, y_2, \ldots, y_n\}$ to be the responses at sample points. Therefore, the regression part can be written as a $n \times p$ model matrix F,

$$F = \begin{pmatrix} b_1(x^1) & \cdots & b_p(x^1) \\ \vdots & \ddots & \vdots \\ b_1(x^n) & \cdots & b_p(x^n) \end{pmatrix} \tag{24}$$

whereas the stochastic process is defined using a $n \times n$ correlation matrix Ψ

$$\Psi = \begin{pmatrix} \psi(x^1, x^1) & \cdots & \psi(x^1, x^n) \\ \vdots & \ddots & \vdots \\ \psi(x^n, x^1) & \cdots & \psi(x^n, x^n) \end{pmatrix} \tag{25}$$

where ψ is a correlation function, parameterised by a set of hyperparameters θ. The hyperparameters are again identified by maximum likelihood estimation (MLE). Brief description of MLE is provided towards the end of this section. The prediction mean and prediction variance of are given as:

$$\mu(x) = M\alpha + r(x)\Psi^{-1}(y - F\alpha) \tag{26}$$

and

$$s^2(x) = \sigma^2 \left(1 - r(x)\Psi^{-1} r(x)^T + \frac{\left(1 - F^T \Psi^{-1} r(x)^T\right)}{F^T \Psi^{-1} F} \right) \tag{27}$$

where $M = \left(b_1(x_p) \ldots b_p(x_p)\right)$ is the modal matrix of the predicting point x_p,

$$\alpha = \left(F^T \Psi F\right)^{-1} F^T \Psi^{-1} Y \tag{28}$$

is a $p \times 1$ vector consisting the unknown coefficients determined by generalised least squares regression and

$$r(x) = \left(\psi\left(x_p, x^1\right) \ldots \psi\left(x_p, x^p\right)\right) \tag{29}$$

is an $1 \times n$ vector denoting the correlation between the prediction point and the sample points. The process variance σ^2 is given by

$$\sigma^2 = \frac{1}{n}(Y - F\alpha)^T \Psi^{-1}(Y - F\alpha) \tag{30}$$

Remark 2 Note that the universal Kriging, as formulated above, is an interpolation technique. This can be easily validated by substituting the ith sample point in Eq. (26) and considering that $r(x^i)$ is the ith column of ψ:

$$\mu\left(\mathrm{x}^i\right) = M\alpha + y^i - M\alpha = y^i \tag{31}$$

Remark 3 One issue associated with the universal Kriging is selection of the optimal polynomial order. Conventionally,

the order of the polynomial is selected empirically. As the consequence, the Kriging surrogate formulated may not be optimal.

3.3 Blind Kriging

This variant of Kriging incorporates the Bayesian feature selection method into the framework of universal Kriging. The basic goal is to efficiently determine the basis function b_i that captures the maximum variance in the sample data. To this end, a set of candidate function is considered from which to choose from. In the ideal scenario, the trend function completely represents the sample data and the stochastic process has no influence. However, this is an extremely rare event.

Suppose an existing Kriging model $Y(x)$ with a constant regression function is already available. The basic idea of blind Kriging is to incorporate new features into the regression function of the Kriging surrogate. To this end, the whole set of candidate function c_i is used to fit the data in a linear model as:

$$y(x) = \sum_{i=1}^{p} a_i b_i(\mathrm{x}) + \sum_{i=1}^{t} \beta_i c_i(\mathrm{x}) \tag{32}$$

where t is the number of candidate functions. The first part of Eq. (32) is the regression function considered in Kriging surrogate and therefore, the unknown coefficients a can be determined independent of the β. In blind Kriging, the estimates of β can be considered as the weights associated with the candidate functions. One alternative for determining β is the conventional least-square solution. However, this may yield erroneous result specifically in cases where number of candidate feature is more than the number of samples available. As an alternative, a Gaussian prior distribution is introduced for β,

$$\beta \sim \mathcal{N}\left(0, \sigma_b^2\right) \tag{33}$$

Moreover, the choice of correlation function is restricted to the product correlation form:

$$\psi(x, x') = \prod_{i=1}^{d} \psi_j\left(\left|x_j - x_j'\right|\right) \tag{34}$$

The variance–covariance matrix R can be constructed as:

$$R_j = U_j^{-1} \psi_j \left(U_j^{-1}\right)^T \tag{35}$$

From Eqs. (34) and (35), it is evident that the number of considered features can be chosen per dimension and afterwards the full matrix R is obtained as:

$$\mathbf{R} = \bigotimes_{j=1}^{d} R_j \tag{36}$$

Once the correlation matrix R is constructed, the posterior of β is estimated as:

$$\hat{\beta} = \frac{\sigma_b^2}{\sigma^2} \mathbf{R} \mathbf{M}_c^T \Psi^{-1} (\mathbf{y} - \mathbf{M}\mathbf{a}) \tag{37}$$

where $\mathbf{M}_c$ is the model matrix of all the candidate variable and $\mathbf{M}$ is the model matrix of all currently chosen variables and ψ is the correlation matrix of the samples. The coefficient $\hat{\beta}$ obtained using the proposed approach quantifies the importance of the associated candidate feature. The advantage of the proposed approach, over other available alternatives, is mainly threefold. Firstly, the Bayesian approach proposed utilizes the already available data, making the procedure computationally efficient. Secondly, the variable selection method satisfies the hierarchy criteria. As per this effect, the lower order effects should be chosen before higher order effect. Last, but not the least, the heredity criteria is also satisfied. As per this criteria, an effect cannot be important unless its parent effect is also important.

3.4 Co-Kriging

The fourth variant of Kriging, proposed by Kennedy et al. [101], is known as Co-Kriging. Co-Kriging utilizes the correlation between fine and course model data to enhance the prediction accuracy. Unlike other variants of Kriging, Co-Kriging can be utilized for multi-fidelity analysis. Moreover, computational cost (in terms of CPU time) is significantly less for Co-Kriging, as compared to the other variants.

Suppose $X_c = \left\{x_c^1, \ldots, x_c^{n_c}\right\}$ and $X_e = \left\{x_e^1, \ldots, x_e^{n_e}\right\}$ be the low-fidelity and high-fidelity sets of sample points. The associate functions are denoted by $y_c = \left\{y_c^1, \ldots, y_c^{n_c}\right\}$ and $y_e = \left\{y_e^1, \ldots, y_e^{n_e}\right\}$. Creating a Co-Kriging model can be interpreted as constructing two Kriging models in sequence. In the first step, a Kriging model $Y_C(x)$ of the course data (X_c, y_c) is constructed. Subsequently, the second Kriging model $Y_D(x)$ is constructed on the residuals on the residuals of the fine and course data (X_e, y_d), where

$$y_d = y_e - \rho \mu_c(X_e) \tag{38}$$

where $\mu(X_e)$ is obtained using Eq. (26). The parameter ρ is estimated as part of the MLE of the second Kriging model. It is to be noted that the choice of the correlation function and regression function of both the Kriging model can be adjusted separately. The resulting Co-Kriging model is represented using Eq. (26), where $r(x)$ and Ψ are written as functions of two separate Kriging models:

$$r(x) = \begin{pmatrix} \rho\sigma_c^2 r_c(x) & \rho\sigma_c^2 r_c\left(x, X_f\right) + \sigma_d^2 r_d(x) \end{pmatrix} \tag{39}$$

and

$$\Psi = \begin{pmatrix} \sigma_c^2 \Psi_c & \rho\sigma_c^2 \Psi_c(X_c, X_f) \\ 0 & \rho\sigma_c^2 \Psi_c(X_f, X_f) + \sigma_d^2 \Psi_d \end{pmatrix} \tag{40}$$

where $(F_c, \sigma_c, \Psi_c, M_c)$ and $(F_d, \sigma_d, \Psi_d, M_d)$ are obtained from $Y_C(x)$ and $Y_D(x)$. Similarly σ_c and σ_d are the process variance and $\Psi_c(\cdot,\cdot)$ and $\Psi_d(\cdot,\cdot)$ are correlation matrices of $Y_C(x)$ and $Y_D(x)$ respectively.

3.5 Stochastic Kriging

Although the interpolation property of Kriging is advantageous while dealing with deterministic simulation problems, it often yields erroneous results for problems involving uncertainties/noise. In order to address this issue, stochastic Kriging has been developed. In stochastic Kriging, the noise is modelled as a separate Gaussian process $\xi(x)$ with zero mean and covariance Σ. The stochastic Kriging predictor thus becomes:

$$\hat{y}(x) = M\alpha + r(x)\left(\Psi + \frac{1}{\sigma^2}\Sigma\right)^{-1}(\bar{y} - F\alpha) \tag{41}$$

where $\frac{1}{\sigma^2}\Sigma$ is a matrix resembling noise-to-signal ratios and $\bar{y}$ is a vector containing the average function values of the repeated simulations for each sample. Note that if the entries of Σ are zero, Eq. (41) converges to Eq. (26).

The covariance matrix Σ for noise can have various forms. In stochastic simulation, Σ is created based on repeated simulation. In the simplest form, Σ takes the following form:

$$\Sigma = \begin{pmatrix} \mathrm{var}(y^1) & \cdots & 0 \\ \vdots & \ddots & \vdots \\ 0 & \cdots & \mathrm{var}(y^1) \end{pmatrix} \tag{42}$$

where $\mathrm{var}(y^i)$ is the variance between the repeated simulation of data point i. On contrary, if the problem under consideration is deterministic (but noisy), Σ consists of scalar values 10^{λ} on its diagonal. The variable λ is estimated as part of the likelihood optimization of the Kriging.

3.6 Correlation Function

All the variants of Kriging are dependent on the choice of correlation function to create an accurate surrogate. Various type of correlation function is available in literature [102–104]. In this work, we restrict ourselves to the stationary correlation function defined as:

$$\psi(x, x') = \prod_j \psi_j(\theta, x_i - x_i') \tag{43}$$

The correlation function defined in Eq. (43) has two desirable properties. Firstly, the correlation function for multivariate functions can be represented as product of one dimensional correlations. Secondly, the correlation is stationary and depends only in the distance between two points. Various correlation function that satisfies Eq. (43) is available in literature. In this study, seven correlation functions, namely (a) exponential correlation function, (b) generalised exponential correlation function (c) Gaussian correlation function (d) linear correlation function (e) spherical correlation function (f) cubic correlation function and (g) spline correlation function has been investigated. The mathematical forms of all the correlation functions are provided below:

(a) Exponential correlation function

$$\psi_j(\theta; d_j) = \exp(-\theta_j |d_j|) \tag{44}$$

(b) Generalised exponential correlation function

$$\psi_j(\theta; d_j) = \exp\left(-\theta_j |d_j|^{\theta_{n+1}}\right), \quad 0 < \theta_{n+1} \le 2 \tag{45}$$

(c) Gaussian correlation function

$$\psi_j(\theta; d_j) = \exp\left(-\theta_j d_j^2\right) \tag{46}$$

(d) Linear correlation function

$$\psi_j(\theta; d_j) = \max\{0, 1 - \theta_j |d_j|\} \tag{47}$$

(e) Spherical correlation function

$$\psi_j(\theta; d_j) = 1 - 1.5\xi_j + 0.5\xi_j^2,\ \xi_j = \min\{1, \theta_j |d_j|\} \tag{48}$$

(f) Cubic correlation function

$$\psi_j(\theta; d_j) = 1 - 3\xi_j^2 + 2\xi_j^3,\ \xi_j = \min\{1, \theta_j |d_j|\} \tag{49}$$

(g) Spline correlation function

$$\psi_j(\theta; d_j) = \begin{cases} 1 - 5\xi_j^2 + 30\xi_j^3, & 0 \le \xi_j \le 0.2 \\ 1.25\left(1 - \xi_j^3\right), & 0.2 \le \xi_j \le 1 \\ 0, & \xi_j > 1 \end{cases} \tag{50}$$

where $\xi_j = \theta_j |d_j|$

For all the correlation functions described above, $d_j = x_i - x_i'$.

3.7 Maximum Likelihood Estimation (MLE)

Another important aspect of all Kriging surrogate is determination of the hyperparameters governing the correlation functions. The conventional way of determining the hyperparameters is by employing the maximum likelihood estimate (MLE). There are several variants of likelihood that one can utilize. In this study, we limit our

discussion to marginal likelihood and Pseudo likelihood only.

3.7.1 Marginal Likelihood

The natural log of the marginal likelihood is given as:

$$\log\left(\mathcal{L}_{\text{marginal}}\right) = \frac{n}{2}\log(2\pi) + \frac{n}{2}\log\left(\sigma^2\right) + \frac{1}{2}\log(|\Psi|) + \frac{1}{2\sigma^2}(y - F\alpha)^T \Psi^{-1}(y - F\alpha) \tag{51}$$

Equation (51) is simplified by taking derivatives with respect to α and σ^2 and equating to zero. $\frac{n}{2}\log(\sigma^2)$ in Eq. (51) denotes the quality of fit. Similarly, $\frac{1}{2}\log(|\Psi|)$ denotes the complexity penalty. Therefore, the marginal likelihood automatically balances flexibility and accuracy. It is to be noted that marginal likelihood depends on correct specification of Kriging model for the data and hence, may not be robust enough when Kriging model is misspecified.

3.7.2 Pseudo Likelihood

In order to address the robustness issue of marginal likelihood, the pseudo likelihood has emerged as an attractive alternative. The pseudo likelihood estimate is given as:

$$\log(\mathcal{L}_{PL}) = \sum_{i=1}^{n} -\frac{1}{2}\log\left(\sigma_i^2\right) - \frac{\left(y_i - F\alpha - \mu^i\right)^2}{2\sigma_i^2} - \frac{1}{2}\log(2\pi) \tag{52}$$

where

$$\mu^i = y^i - F\alpha - \frac{\Psi^{-1}y}{\Psi_{ii}^{-1}} \tag{53}$$

and

$$\sigma_i^2 = \frac{1}{\Psi_{ii}^{-1}} \tag{54}$$

Since pseudo likelihood is independent of the model selection and hence, yields a more robust solution.

4 Stochastic Approach Using Kriging Model

The stocasticity in material properties of laminated composite shallow doubly curved shells, such as longitudinal elastic modulus, transverse elastic modulus, longitudinal shear modulus, transverse shear modulus, Poisson's ratio, mass density and geometric properties such as ply-orientation angle as input parameters are considered for the uncertain natural frequency analysis. In the present study, frequency domain feature (first three natural frequencies) is considered as output. It is assumed that the distribution of randomness for input parameters exists within a certain band of tolerance with respect to their deterministic mean values following a uniform random distribution. In present investigation, $\pm 10°$ for ply orientation angle with subsequent $\pm 10\,\%$ tolerance for material properties from deterministic mean value are considered for numerical illustration. For the purpose of comparative assessment of different Kriging model variants, both low and high dimensional input parameter space is considered to address the issue of dimensionality in surrogate modelling. For low dimensional input parameter space, stochastic variation of layer-wise ply orientation angles $\{\theta(\bar{\omega})\}$ are considered, while combined variation of all aforementioned layer-wise stochastic input parameters $\{g(\bar{\omega})\}$ are considered to explore the relatively higher dimensional input parameter space as follows:

Case-1 Variation of ply-orientation angle only: $\theta(\bar{\omega}) = \{\theta_1\theta_2\theta_3 \ldots \theta_i \ldots \theta_l\}$.

Case-2 Combined variation of ply orientation angle, elastic modulus (longitudinal and transverse), shear modulus (longitudinal and transverse), Poisson's ratio and mass density:

$$g\{\theta(\bar{\omega}), \rho(\bar{\omega}), G_{12}(\bar{\omega}), G_{23}(\bar{\omega}), E_1(\bar{\omega})\} = \left\{ \begin{array}{l} \Phi_1(\theta_1 \ldots \theta_l), \Phi_2(E_{1(1)} \ldots E_{1(l)}), \Phi_3(E_{2(1)} \ldots E_{2(l)}), \Phi_4(E_{12(1)} \ldots E_{12(l)}), \\ \Phi_5(E_{23(1)} \ldots E_{23(l)}), \Phi_6(\mu_1 \ldots \mu_l), \Phi_7(\rho_1 \ldots \rho_l) \end{array} \right\}$$

where θ_i, $E_{1(i)}$, $E_{2(i)}$, $G_{12(i)}$, $G_{23(i)}$, μ_i and ρ_i are the ply orientation angle, elastic modulus along longitudinal and transverse direction, shear modulus along longitudinal direction, shear modulus along transverse direction, Poisson's ratio and mass density, respectively and 'l'

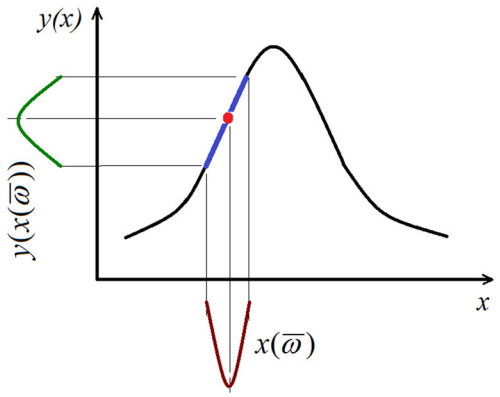

Fig. 3 Stochastic simulation model

denotes the number of layer in the laminate. $\bar{\omega}$ represents the stochastic character of the input parameters. In the present investigation a 4 layered composite laminate is considered having total 4 and 28 random input parameters for individual and combined variations respectively. Figure 3 shows a schematic representation of the stochastic system where x and $y(x)$ are the collective input and output parameters with stochastic character respectively. Latin hypercube sampling [74] is employed in this study for generating sample points to ensure the representation of all portions of the vector space. In Latin hypercube sampling, the interval of each dimension is divided into m non-overlapping intervals having equal probability considering a uniform distribution, so the intervals should have equal size. Moreover, the sample is chosen randomly from a uniform distribution a point in each interval in each dimension and the random pair is selected considering equal likely combinations for the point from each dimension. Figure 4 represents the Kriging based uncertainty quantification algorithm wherein the actual finite element model of composite shell is effectively replaced by the computationally efficient Kriging models and subsequently comparative performance of different Kriging variants are judged on the basis of accuracy and computational efficiency.

5 Results and Discussion

In this section, the performance of the Kriging variants for stochastic free vibration analysis of laminated composite shells has been investigated. Two different cases of stochastic variations have been considered for individual and combined stochasticity having 4 and 28 random input parameters respectively, as discussed in the previous section. Apart from the performance of the Kriging variants, the effect of covariance functions has been illustrated. The

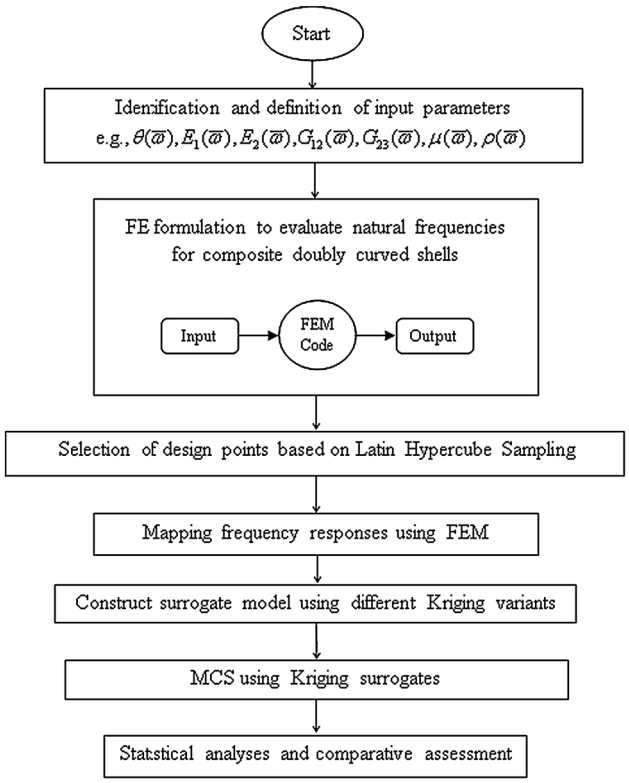

Fig. 4 Flowchart of stochastic natural frequency analysis using Kriging model variants

two alternatives for computing the hyperparameters invovled in Kriging based surrogate, namely the maximum likelihood estimate and pseudo likelihood estimate, have also been illustrated. Additionally, stochastic Kriging has been utilized to investigate the effect of variance noise levels present in the system. For all the cases, results obtained are bechmarked against crude MCS results considering 10,000 realizations in each case. For full scale MCS, number of original FE analysis is same as the sampling size.

5.1 Validation

A four layered graphite-epoxy symmetric angle-ply (45°/−45°/−45°/45°) laminated composite cantilever shallow doubly curved hyperbolic paraboloid ($R_x/R_y = -1$) shell has been considered for the analysis. The length, width and thickness of the composite laminate considered in the present analysis are 1 m, 1 mm and 5 mm, respectively. Material properties of graphite–epoxy composite [45] considered with deterministic mean value as $E_1 = 138.0$ GPa, $E_2 = 8.96$ GPa, $\nu_{12} = 0.3$, $G_{12} = 7.1$ GPa, $G_{13} = 7.1$ GPa, $G_{23} = 2.84$ GPa, $\rho = 3202$ kg/m^3. A typical discretization of (6 × 6) mesh on plan area with 36 elements and 133 nodes with natural coordinates of an

Table 1 Non-dimensional fundamental natural frequencies [$\omega = \omega_n L^2 \sqrt{(\rho/E_1 h^2)}$] of three layered [θ/−θ/θ] graphite–epoxy twisted plates, L/b = 1, b/h = 20, ψ = 30°

Ply-orientation angle, θ	Present FEM (with mesh size)					Qatu and Leissa [46]
	4 × 4	6 × 6	8 × 8	10 × 10	12 × 12	
15°	0.8588	0.8618	0.8591	0.8543	0.8540	0.8759
30°	0.6753	0.6970	0.6752	0.6722	0.6717	0.6923
45°	0.4691	0.4732	0.4698	0.4578	0.4575	0.4831
60°	0.3189	0.3234	0.3194	0.3114	0.3111	0.3283

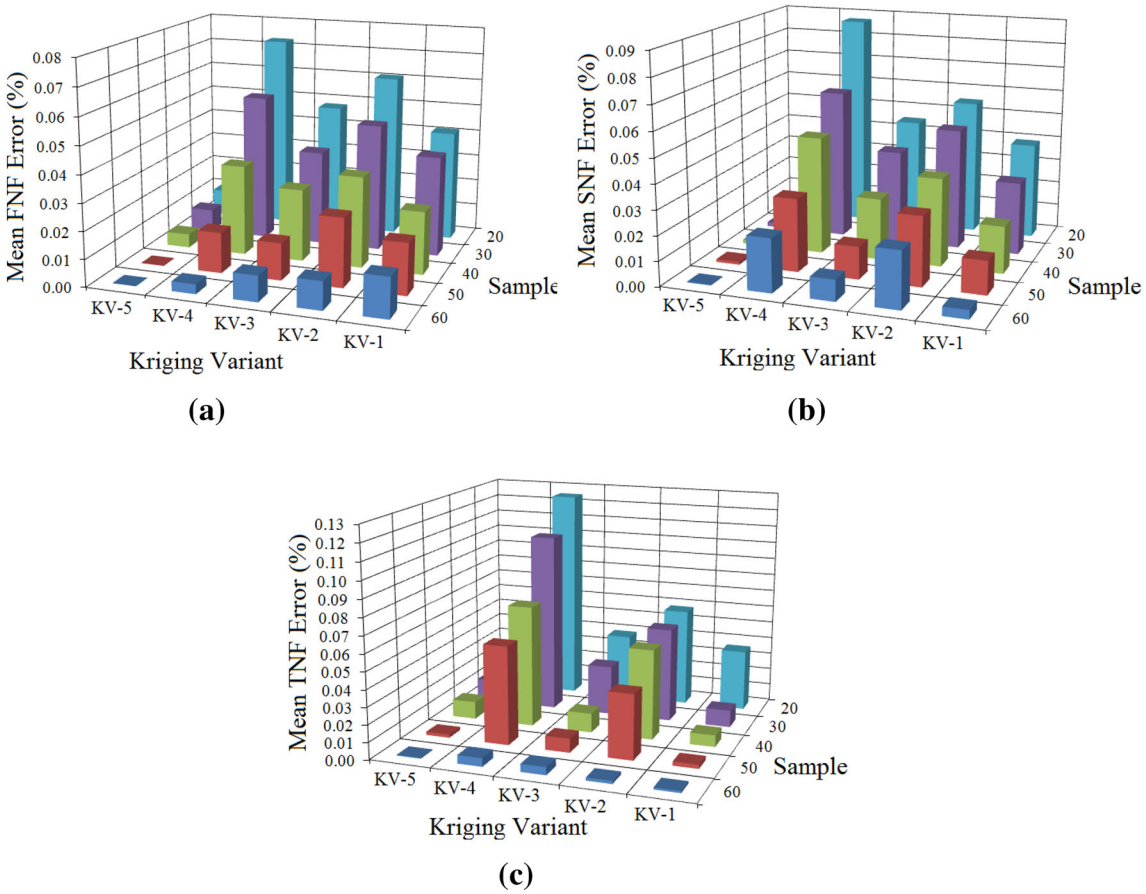

Fig. 5 Error of the Kriging variants in predicting the mean error (%) of first three natural frequencies for the first case (individual variation). **a** Mean first natural frequency (FNF) error. **b** Mean second natural frequency (SNF) error. **c** Mean third natural frequency (TNF) error

isoparametric quadratic plate bending element has been considered for the present FEM approach. The finite element code is validated with the results available in the open literature as shown in Table 1 [46]. Convergence studies are performed using mesh division of (4 × 4), (6 × 6), (8 × 8), (10 × 10) and (12 × 12) wherein (6 × 6) mesh is found to provide best results with the least difference compared to benchmarking results [46]. The marginal differences between the results by Qatu and Leissa [46] and the present finite element approach can be attributed to consideration of transverse shear deformation and rotary inertia and also to the fact that Ritz method overestimates the structural stiffness of the composite plates.

5.2 Comparative Assessment of Krigng Variants

In this section the performance of the Kriging variants in stochastic free vibration analysis of FRP composite shells has been presented. For the ease of understanding and refering, following notations have been used hereafter:

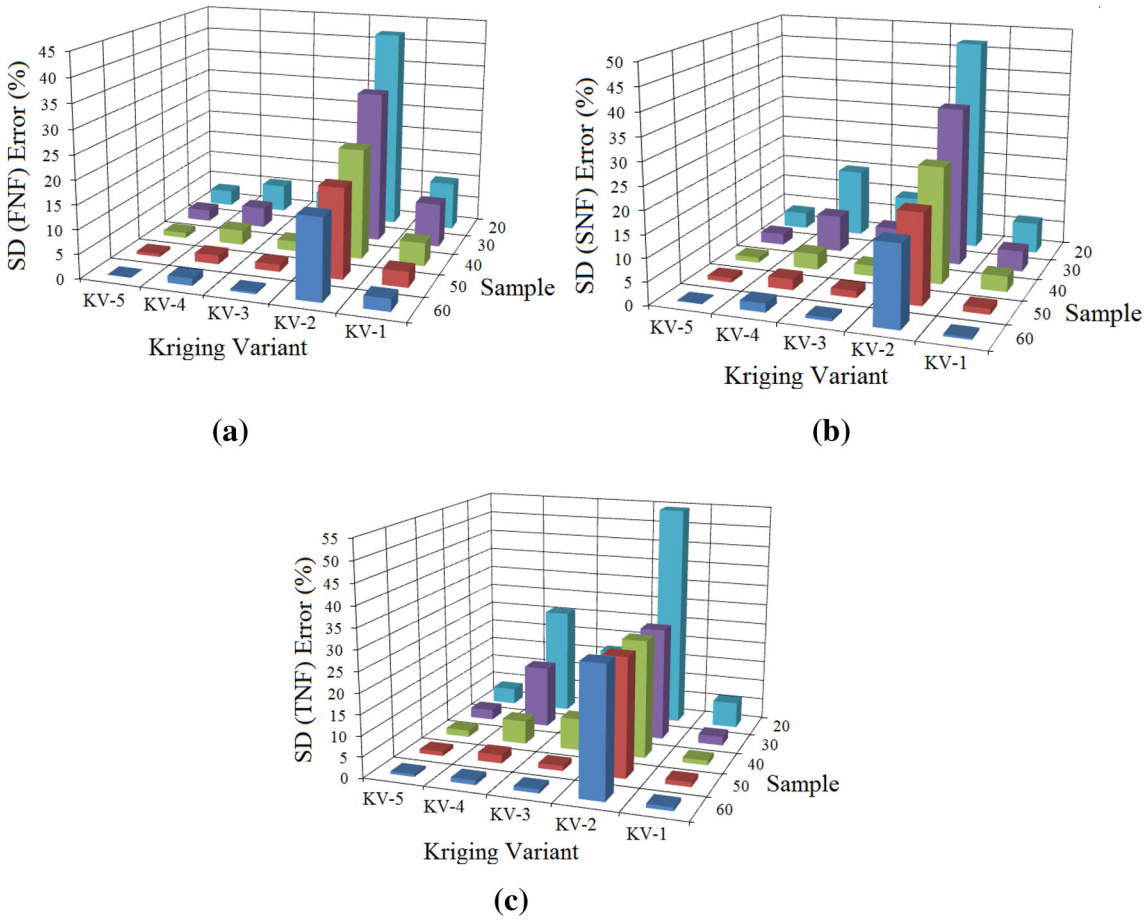

Fig. 6 Error of the Kriging variants in predicting the standard deviation error (%) of first three natural frequencies for the first case (individual variation). **a** Standard deviation (SD) FNF error. **b** Standard deviation (SD) SNF error. **c** Standard deviation (SD) TNF error

(a) KV1: ordinary Kriging.
(b) KV2: universal Kriging with pseudo likelihood estimate.
(c) KV3: blind Kriging.
(d) KV4: Co-Kriging.
(e) KV5: stochastic Kriging with zero noise (Universal Kriging based on marginal likelihood estimator).

In addition to the above, individual and combined variation of input paramenters as described in Sect. 4, are implied as first and second case throughout this article. For the first case (i.e., uncertainties in ply orientation angles only), the sample size is varied from 20 to 60 at an interval of 10. Figures 5 and 6 show the mean and standard deviation of error, corresponding to the first three natural frequencies. For all the three frequencies, KV5 yields the best results. Performance of the other Kriging variants varies from case to case. For instance, results obtained using KV4 outperforms all but KV5 in predicting the mean of first natural freuency. However, for the mean of second natural frequencies, KV4 yields the worst results. Similarly arguments hold for KV1 and KV3 as well. KV2, in most of the cases (specifically for standard deviation of response), yields erroneous results. This is probably due to the inability of the pseudo likelihood function to accurately predict the hyperparameters associated with the covariance function. Probability density function (PDF) and representative scatter plot of the first three natural frequencies, obtained using the Kriging variants and crude MCS, are shown in Figs. 7 and 8. KV5 yields the best result followed by KV4 nd KV3. Results obtained using KV2 is found to be eroneous. As already stated, this is due to erroneous hyperparameters obtained using the pseudo likelihood estimate.

For the second case (combined variation of all input parameters), the sample size is varied from 250 to 600 at an interval of 50. Figures 9 and 10 show the error in mean and standard deviation of the first three natural frequencies obtained using the five variants of Kriging. For mean natural frequencies, all but KV2 yields excellent results with extremely low error. However, for standard deviation of

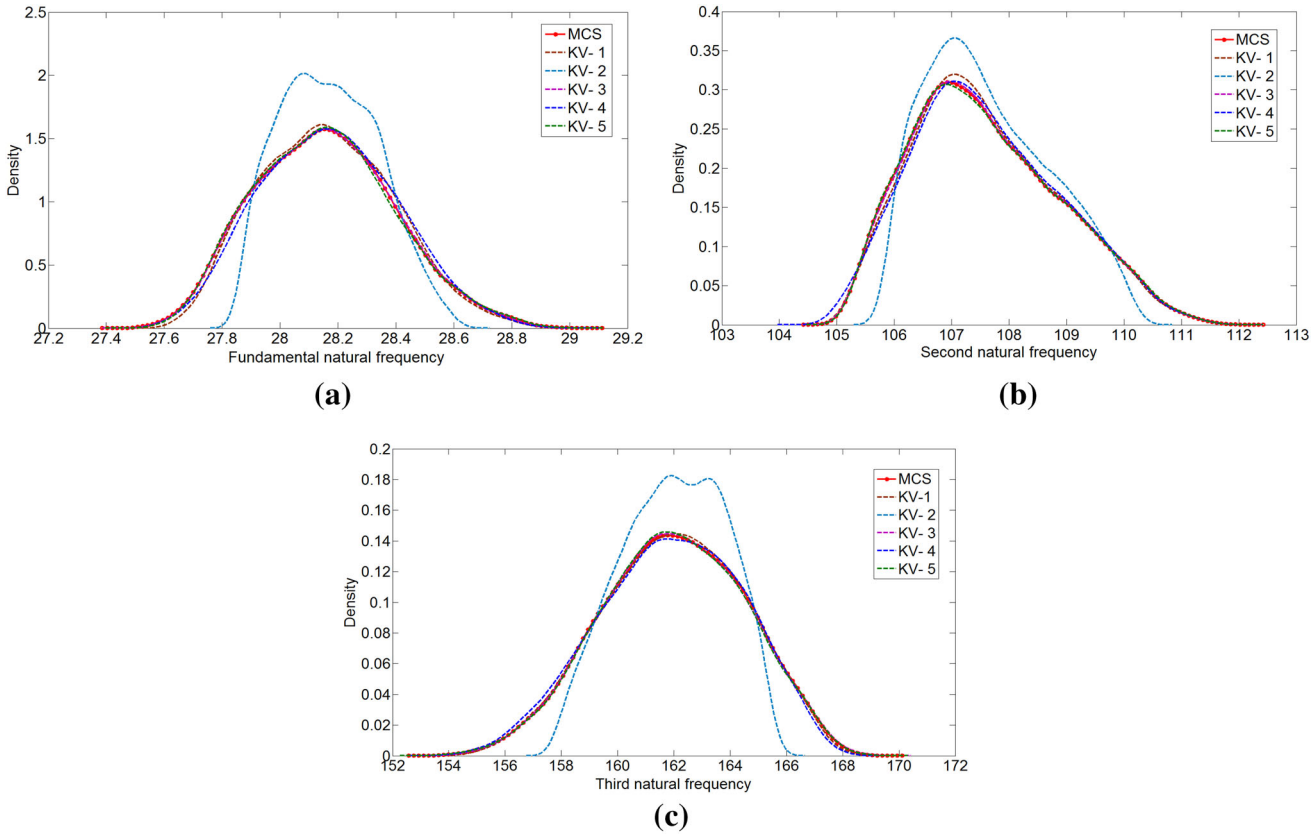

Fig. 7 PDF of first three natural frequencies for the first case (individual variation) obtained using the Kriging variants (50 samples) and MCS. **a** PDF of first natural frequency. **b** PDF of second natural frequency. **c** PDF of third natural frequency

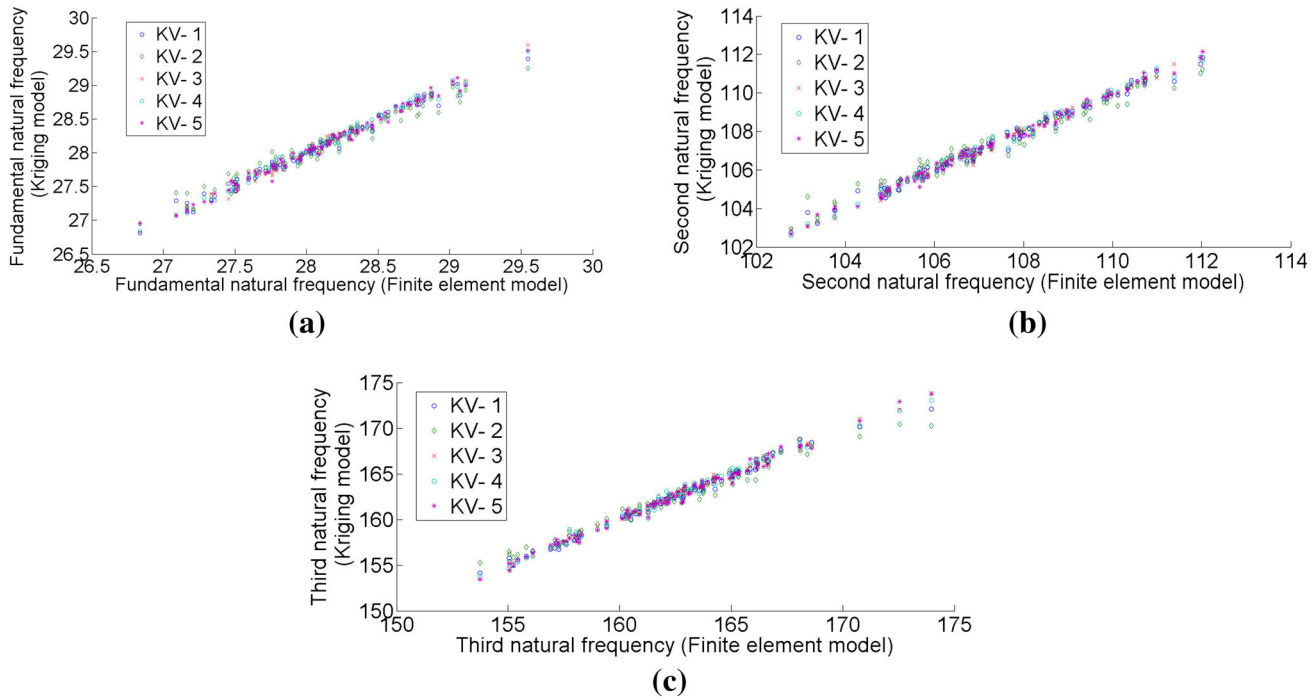

Fig. 8 *Scatter plot* for the first three natural frequencies for the first case (individual variation) obtained using 50 samples. **a** *Scatter plot* for first natural frequency. **b** *Scatter plot* for second natural frequency. **c** *Scatter plot* for third natural frequency

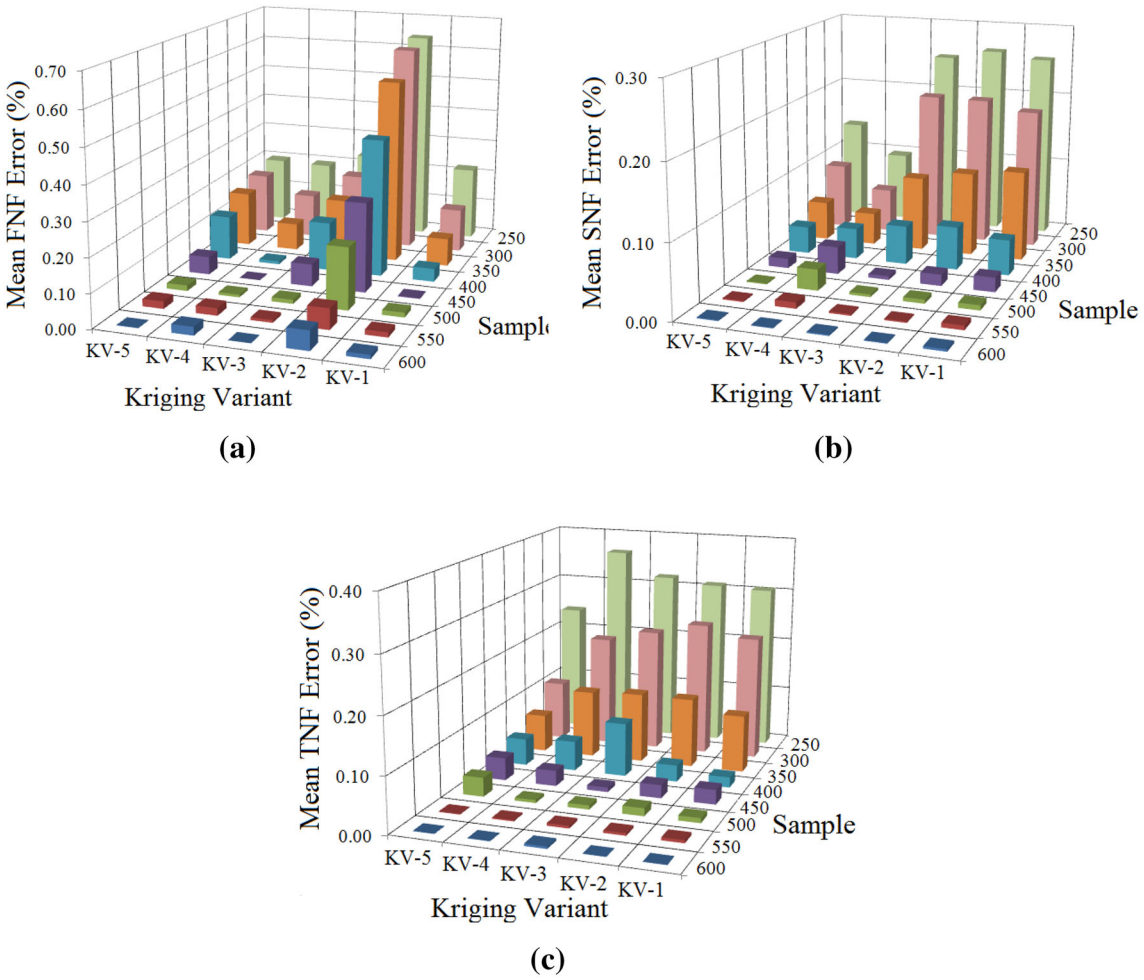

Fig. 9 Error of the Kriging variants in predicting the mean of first three natural frequencies for the second case (combined variation). **a** Mean first natural frequency (FNF) error. **b** Mean second natural frequency (SNF) error. **c** Mean third natural frequency (TNF) error

the first two natural frequencies ordinary Kriging (KV1) yields erroneous results. Similar to previous case, KV3, KV4 and KV5 are found to yield excellent results with extremely low prediction error. PDF plot and representative scatter plot of the first three natural frequency, obtained using the Kriging variants and crude MCS, are shown in Figs. 11 and 12 respectively. Apart from KV2, all the variants are found to yield excellent results.

It is worthy to mention here that the whole point of using a Kriging based uncertainty quantification approach is to achieve computational efficiency in terms of finite element simulation. For example, the probabilistic descriptions and statistical results of the natural frequencies presented in this study are based on 10,000 simulations. In case of crude MCS, same number of actual finite element simulations are needed to be carried out. However, in the present approach of Kriging based uncertainty quantification, the number of actual finite element simulations needed is same as sample size to construct the Kriging models. Thus, if 50 and 550 samples are required to form the Kriging models for the individual and combined cases respectively, the corresponding levels of computational efficiency are about 200 times and 18 times with respect to crude MCS. Except the computational time associated with finite element simulation as discussed above, another form of significant computational time involved in the process of uncertainty quantification can be the building and prediction for the Kriging models. In general, the computational expenses are found to increase for higher dimension of the input parameter space. The second form of computational time can be different for different Kriging variants. A comparative investigation on the computational times for different Kriging model variants are provided next.

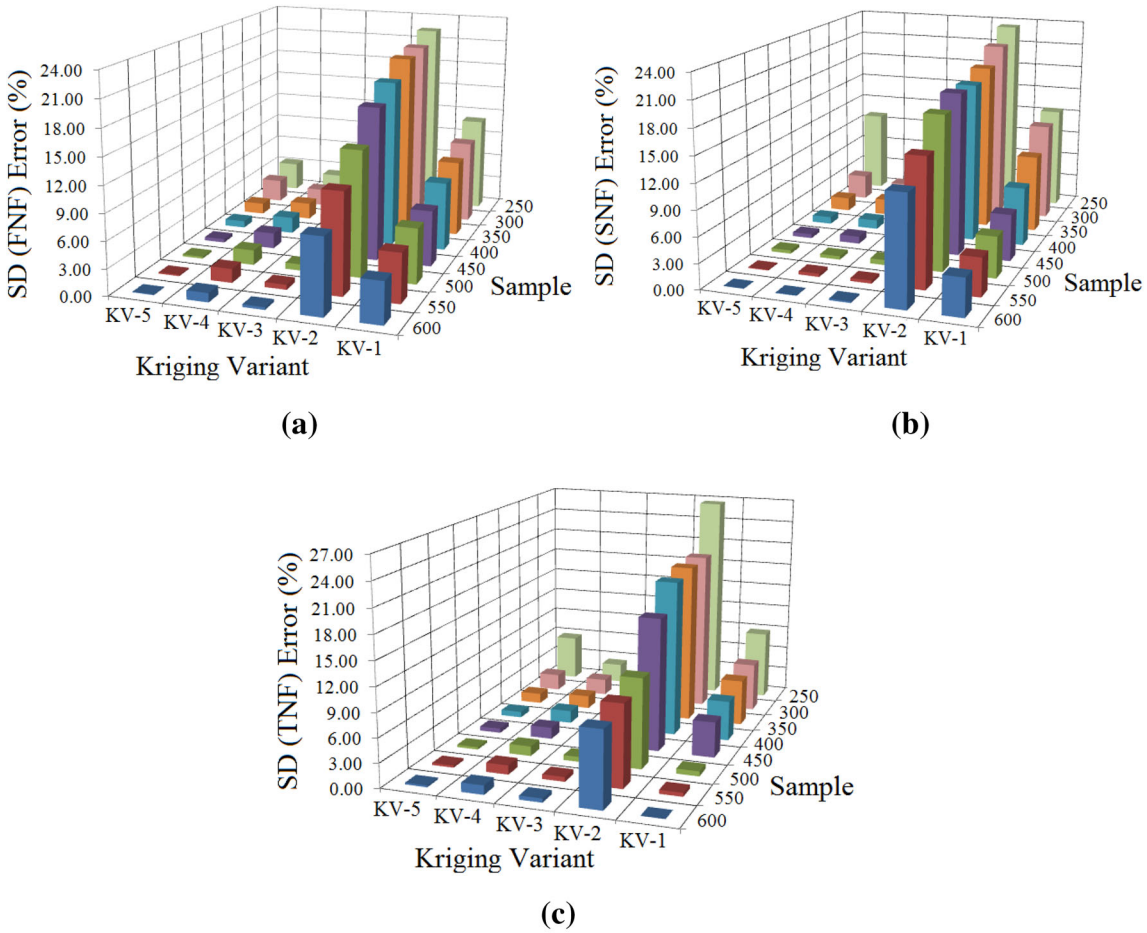

Fig. 10 Error of the Kriging variants in predicting the standar deviation of first three natural frequencies for the second case (combined variation). **a** Standard deviation (SD) FNF error. **b** Standard deviation (SD) SNF error. **c** Standard deviation (SD) TNF error

Table 2 reports the computational time required for Kriging model prediction by the five Kriging variants for both cases. Please note here that the time reported in this table is for building and predictions corresponding to different Kriging models and this time has no relation with the time required for finite elemet simulation of laminated composite shell. It is observed that for individual variation of input paramaeters (4 input parameters), KV1 is the fastest followed by KV5 and KV4. However. For the combined variation case (28 input parameters), KV4 is much faster compared to the other variants. This is because unlike the other variants KV4 first generates a low fidelity solution from comparatively less number of sample points and update it by adding additional sample points. As a consequence, the matrix inversion involved in KV4 becomes less time consiming, making the overall procedure computationally efficient. However, this advantage of KV4 is only visible for large systems, involving large number of input variables (combined variation case). For smaller systems, inverting two matrices, instead of one, may not be advantegeous as observed in the individual variation case.

5.3 Comparative Assessment of Various Covariance Functions

This section investigates the performance of the various covariance functions used in Kriging. To be specific, performance of the following seven covariance functions has been investigated:

(a) COV1: cubic covariance function.
(b) COV2: exponential covariance function.
(c) COV3: Gaussian covariance function.
(d) COV4: linear covariance function.
(e) COV5: spherical covariance function.
(f) COV6: spline covariance function.
(g) COV7: generalised exponential covariance function.

The above mentioned covariance functions have been utilized in conjunction with ordinary Kriging (KV1); the

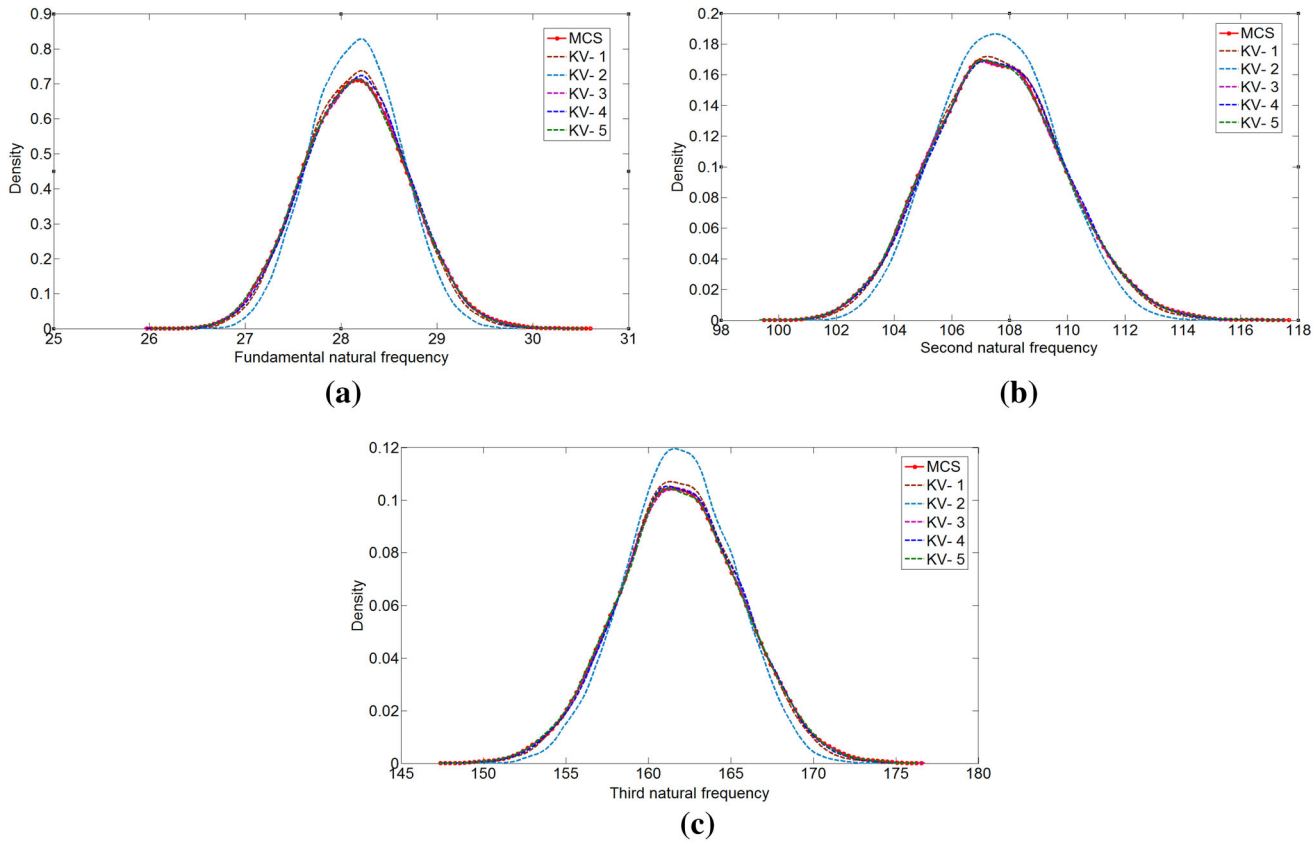

Fig. 11 PDF of first three natural frequencies for the second case (combined variation) obtained using 550 samples. **a** PDF for first natural frequency. **b** PDF for second natural frequency. **c** PDF for third natural frequency

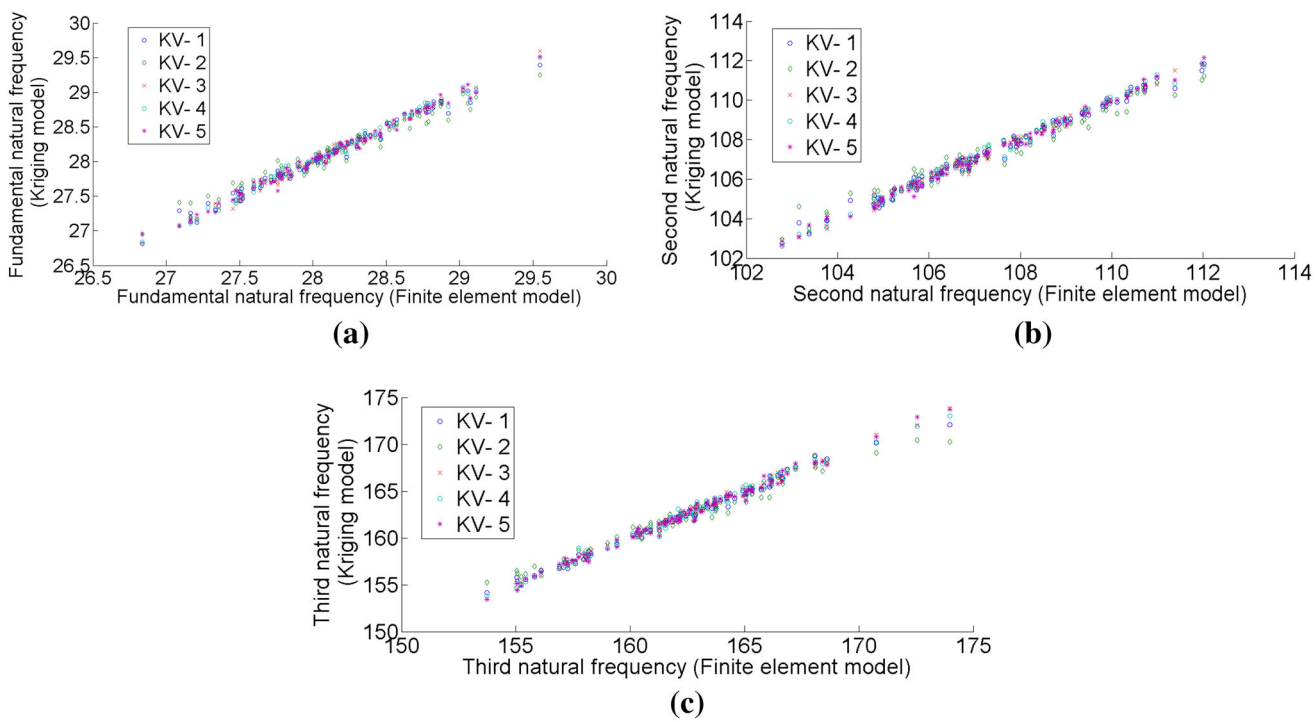

Fig. 12 Scatter plot for the first three natural frequencies for the second case (combined variation) obtained using 550 samples. **a** *Scatter plot* for first natural frequency. **b** *Scatter plot* for second natural frequency. **c** *Scatter plot* for third natural frequency

Table 2 CPU time of the Kriging variants

Number of input parameters	Kriging variants				
	KV1	KV2	KV3	KV4	KV5
First case (individual)	1.0511 s	3.1391 s	1.6714 s	1.62 s	1.2258 s
Second case (combined)	335.4105 s	5205.1 s	7330.1 s	110.9570 s	1031.3 s

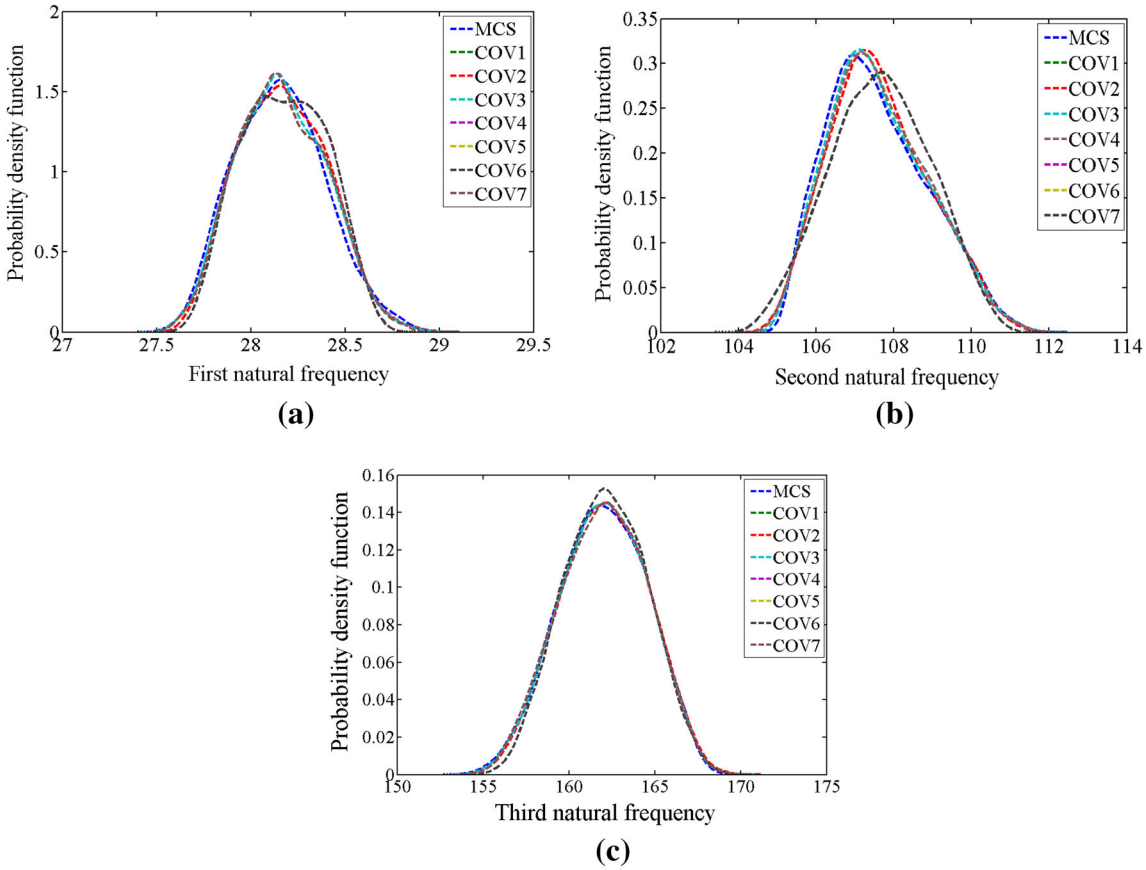

Fig. 13 PDF of the first three natural frequencies for the *first case* obtained using various covariance functions. For all the cases, Kriging based surrogate is formulated using 50 sample points. Ordinary Kriging (KV1) is used in conjunction with the covariance functions. **a** PDF of first natural frequency. **b** PDF of second natural frequency. **c** PDF of third natural frequency

reason being ordinary Kriging does not have a regression part and hence the effect of covariance function will be more prominent in such case. As per the study reported in previous subsection, Kriging based surrogate is formulated with 50 sample points in the first case (individual variation). Figure 13 shows the PDF of response obtained using various covariance functions for the first case. It is observed that for all the three natural frequencies, Gaussian covariance (COV3) yields the best resut followed by exponential (COV2) and generalised exponential (COV7) covariance function. The error (%) in mean and standard deviation of natural frequencies are shown in Figs. 14 and 15. For all the cases, Gaussian, expnential and generalised exponential covariance functions yields the best results. Interestingly, results obtained using cubic (COV1), linear (COV4), spherical (COV5) and spline (COV6) covariance functions are almost identical. Similar results has been observed for the second case (combined variation). However, due to paucity of space, the results for the second case have not been reported in this article.

5.4 Comparative Assessment of Various Noise Levels

In this section, the effect of noise, present within a system, has been simulated using the stochastic Kriging (KV5). The effect of noise in a system can be regarded as considering other sources of uncertainty besides conventional

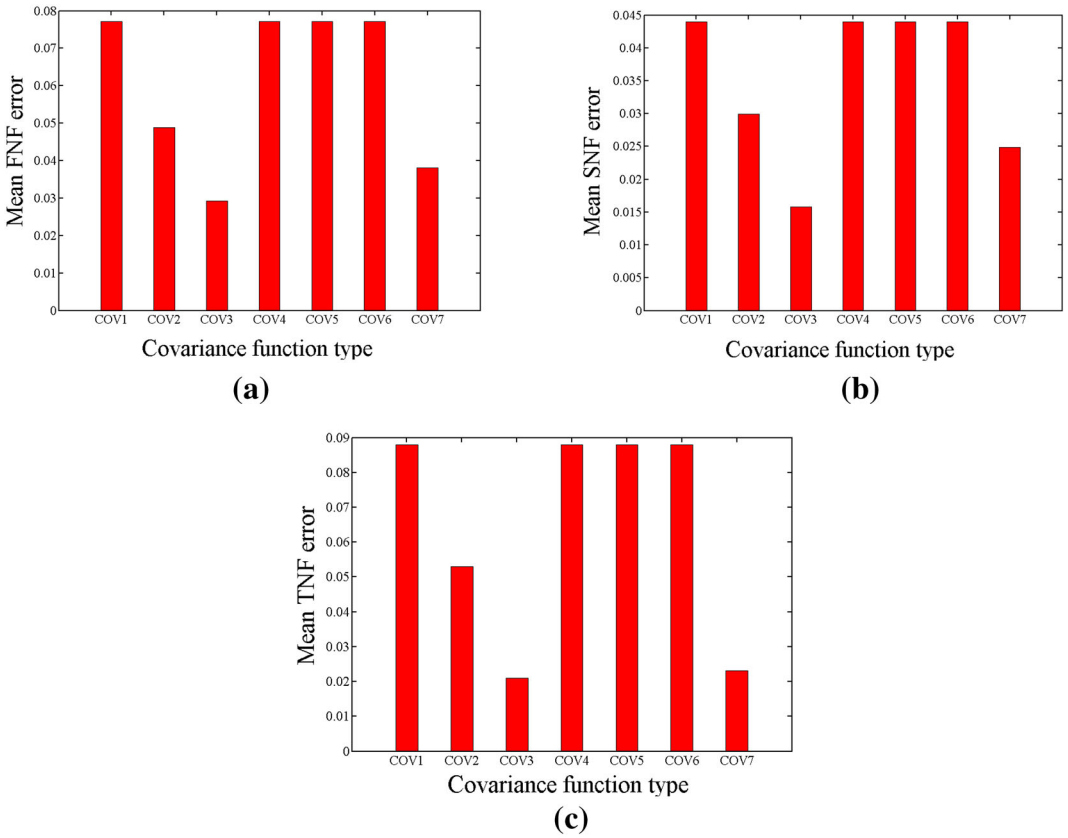

Fig. 14 Error in predicted mean natural frequencies obtained using various covariance functions. **a** Error in predicted mean first natural frequency (FNF). **b** Error in predicted mean second natural frequency (SNF). **c** Error in predicted mean third natural frequency (TNF)

material and geometric uncertainties, viz., error in modelling, human error and various other epistemic uncertainties involved in the system [58, 63, 64, 105, 106]. In present study, gaussian white noise with specific level (p) has been introduced into the output responses as:

$$f_{ijN} = f_{ij} + p\xi_{ij} \tag{55}$$

where f_{ij} denotes the ith frequency in the jth sample in the design point set. The subscript N denotes the frequency in the presence of noise. ξ in Eq. (55) denotes normal distributed random number with zero mean and unit variance. Typical results for the effect of noise have been reported for combined variation of input parameters. Figures 16 and 17 show the representative scatter plots and PDF of the first three natural frequencies corresponding to various noise levels. The distance of the points from diagonal line increases with the increase of noise level in the scatter plots indication lesser prediction accuracy of the Kriging model. Significant change the the standard deviation of the frequencies is observed with changes in the noise level. However, the mean frequencies are found to be mostly insensitive to the noise.

6 Conclusions

This article presents a critical comparative assessment of five Kriging model variants in an exhaustive and comprehensive manner for quantifying uncertainty in the natural frequencies of composite doubly curved shells. Five Kriging variants considered in this study are: Ordinary Kriging, Universal Kriging based on pseudo-likelihood estimator, Blind Kriging, Co-Kriging and Universal Kriging based on marginal likelihood estimator (Stochastic Kriging with zero noise). The comparative assessment has been carried out from the view point of accuracy and computational efficiency. Formulation for finite element modelling of composite shells and Kriging model variants are provided in full depth along with a state-of-the-art review of literature concerning the present investigation. Both low and high dimensional input parameter spaces have been considered in this investigation to explore the effect of dimensionality on different Kriging variants. Results have been presented for different sample sizes to construct the Kriging model variants. A comparative study on performance of different covariant functions has also

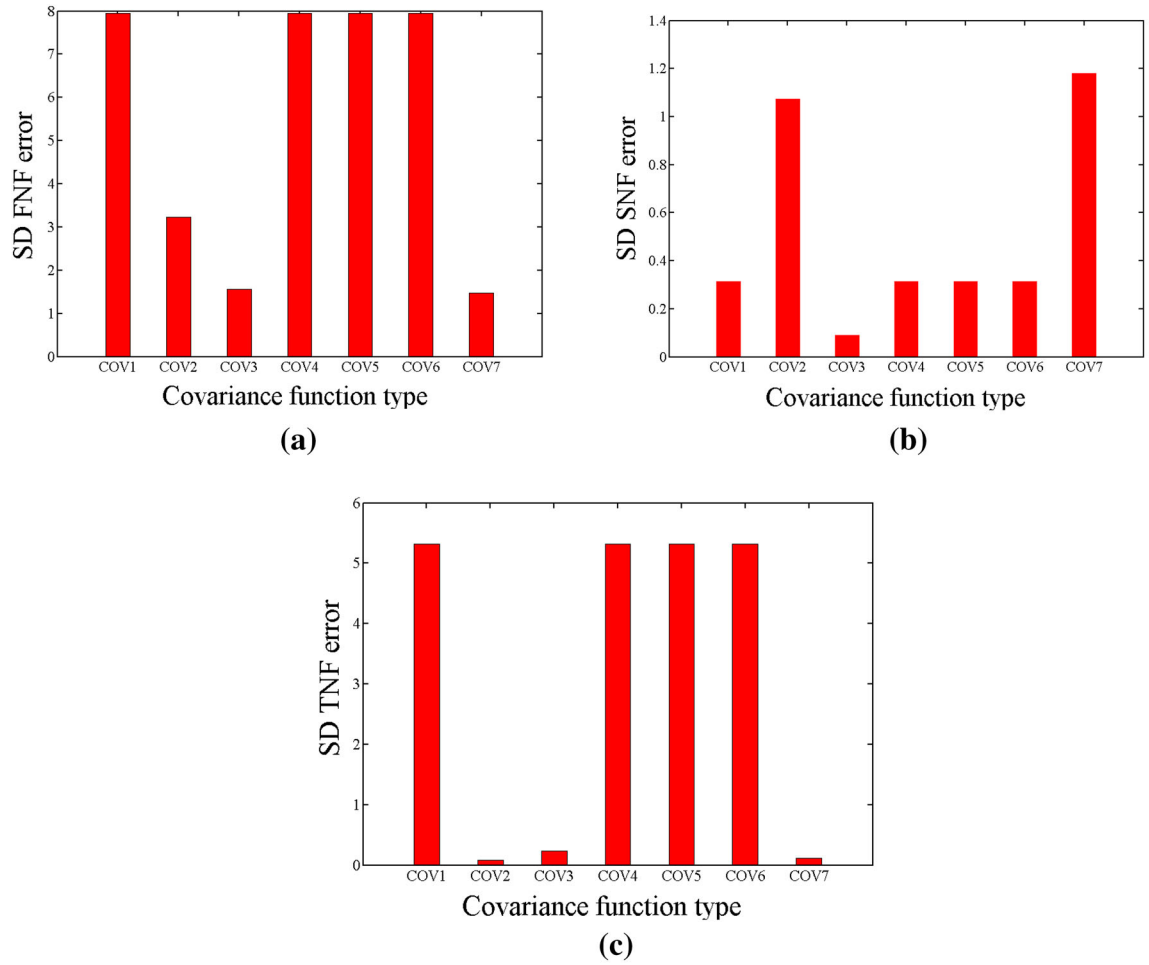

Fig. 15 Error in predicted standard deviation of natural frequencies obtained using various covariance functions. **a** Error in predicted standard deviation of FNF. **b** Error in predicted standard deviation of SNF. **c** Error in predicted standard deviation of TNF

been carried out in conjunction to the present problem. Further the effect of noise has been investigated considering Stochastic Kriging. The major findings of this work are summarized below:

(a) It is observed that Universal Kriging coupled with marginal likelihood estimate yields the best results for both low-dimensional and high-dimensional problems.

(b) Co-Kriging is found to be the fastest in terms of model building and prediction time for high dimensional input parameter space. In case of low dimensional input parameter space, ordinary Kriging is relatively the fastest followed by co-Kriging, blind Kriging and universal Kriging with pseudo likelihood estimate, respectively. However, the effect of relative differences in computational time becomes more crucial for large number of input parameters as considerable amonut of time is required in this case.

(c) Among various covariance functions investigated, it is observed that Gaussian covariance function produces best accuracy.

(d) Last, but not the least, stochastic Kriging is an efficient tool for simulating the effect of noise present in a system. As evident from the results presented, stochastic Kriging yields highly accurate result for system involving certain degree of inherent noise.

The present investigation provides a comprehensive understanding about the performance of different Kriging model variants in surrogate based uncertainty quantification of laminated composite shells. Although this study focuses on stochastic natural frequency analysis of composite shells, the outcomes regarding comparative performance of the Kriging model variants may serve as a valuable reference for different other computationally intensive problems in the broad field of science and engineering.

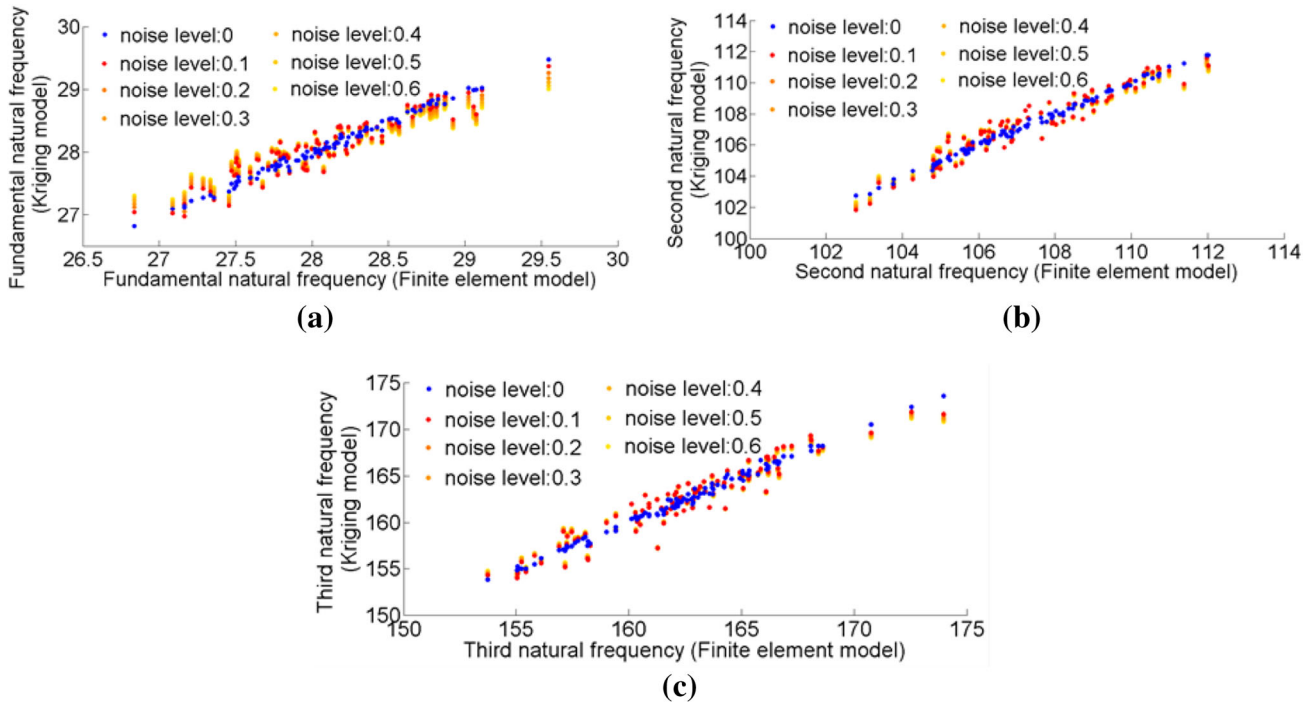

Fig. 16 *Scatter plot* for the first three natural frequencies corresponding to various noise levels. **a** *Scatter plot* for fundamental natural frequency. **b** *Scatter plot* for second natural frequency. **c** *Scatter plot* for third natural frequency

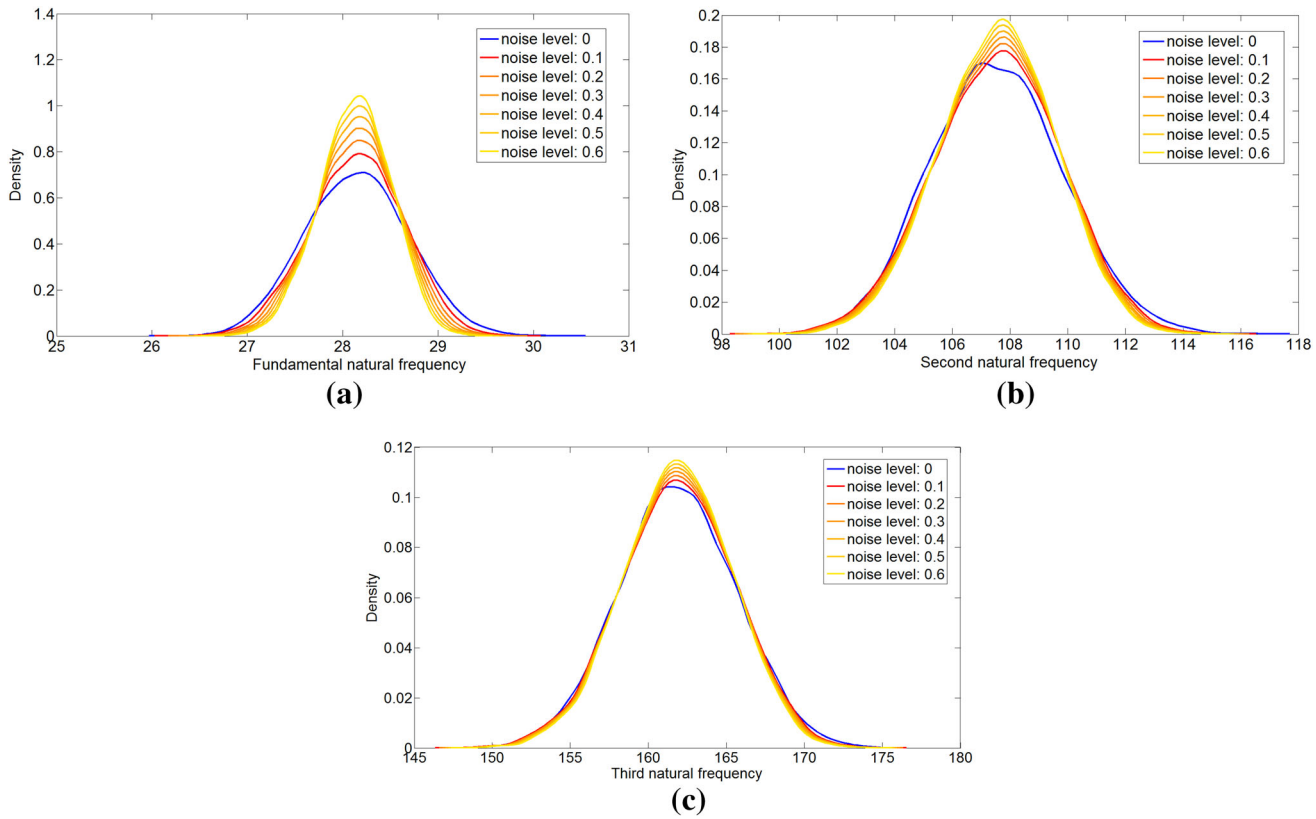

Fig. 17 Probability density function plot for the first three natural frequencies corresponding to various noise levels. **a** PDF for fundamental natural frequency. **b** PDF for second natural frequency. **c** PDF for third natural frequency

Acknowledgments TM acknowledges the financial support from Swansea University through the award of Zienkiewicz Scholarship during the period of this work. SC acknowledges the support of MHRD, Government of India for the financial support provided during this work. SA acknowledges the financial support from The Royal Society of London through the Wolfson Research Merit award. RC acknowledges the support of The Royal Society through Newton Alumni Funding.

References

1. Mallick PK (2007) Fiber-reinforced composites: materials, manufacturing, and design, 3rd edn. CRC Press, Boca Raton
2. Baran I, Cinar K, Ersoy N, Akkerman R, Hattel JH (2016) A review on the mechanical modeling of composite manufacturing processes. Arch Comput Methods Eng. doi:10.1007/s11831-016-9167-2
3. Arregui-Mena JD, Margetts L, Mummery PM (2016) Practical application of the stochastic finite element method. Arch Comput Methods Eng 23(1):171–190
4. Venkatram A (1988) On the use of Kriging in the spatial analysis of acid precipitation data. Atmos Environ (1967) 22(9):1963–1975
5. Fedorov VV (1989) Kriging and other estimators of spatial field characteristics (with special reference to environmental studies). Atm Environ (1967) 23(1):175–184
6. Diamond P (1989) Fuzzy Kriging. Fuzzy Sets Syst 33(3):315–332
7. Carr JR (1990) UVKRIG: a FORTRAN-77 program for universal Kriging. Comput Geosci 16(2):211–236
8. Deutsch CV (1996) Correcting for negative weights in ordinary Kriging. Comput Geosci 22(7):765–773
9. Cressie NAC (1990) The origins of Kriging. Math Geol 22:239–252
10. Matheron G (1963) Principles of geostatistics. Econ Geol 58(8):1246–1266
11. Cressie NAC (1993) Statistics for spatial data: revised edition. Wiley, New York
12. Montgomery DC (1991) Design and analysis of experiments. Wiley, New Jersey
13. Michael JB, Norman RD (1974) On minimum-point second-order designs. Technometrics 16(4):613–616
14. Martin JD, Simpson TW (2005) Use of Kriging models to approximate deterministic computer models. AIAA J 43(4):853–863
15. Lee KH, Kang DH (2006) A robust optimization using the statistics based on Kriging metamodel. J Mech Sci Technol 20(8):1169–1182
16. Sakata S, Ashida F, Zako M (2004) An efficient algorithm for Kriging approximation and optimization with large-scale sampling data. Comput Methods Appl Mech Eng 193:385–404
17. Ryu J-S, Kim M-S, Cha K-J, Lee TH, Choi D-H (2002) Kriging interpolation methods in geostatistics and DACE model. KSME Int J 16(5):619–632
18. Bayer V, Bucher C (1999) Importance sampling for first passage problems of nonlinear structures. Probab Eng Mech 14:27–32
19. Yuan X, Lu Z, Zhou C, Yue Z (2013) A novel adaptive importance sampling algorithm based on Markov chain and low-discrepancy sequence. Aerosp Sci Technol 19:253–261
20. Au SK, Beck JL (1999) A new adaptive importance sampling scheme for reliability calculations. Struct Saf 21:135–138
21. Kamiński B (2015) A method for the updating of stochastic Kriging metamodels. Eur J Oper Res 247(3):859–866
22. Angelikopoulos P, Papadimitriou C, Koumoutsakos P (2015) X-TMCMC: adaptive Kriging for Bayesian inverse modeling. Comput Methods Appl Mech Eng 289:409–428
23. Peter J, Marcelet M (2008) Comparison of surrogate models for turbomachinery design. WSEAS Trans Fluid Mech 3(1):10–17
24. Dixit V, Seshadrinath N, Tiwari MK (2016) Performance measures based optimization of supply chain network resilience: a NSGA-II + Co-Kriging approach. Comput Ind Eng 93:205–214
25. Huang C, Zhang H, Robeson SM (2016) Intrinsic random functions and universal Kriging on the circle. Stat Probab Lett 108:33–39
26. Tonkin MJ, Kennel J, Huber W, Lambie JM (2016) Multi-event universal Kriging (MEUK). Adv Water Resour 87:92–105
27. Kersaudy P, Sudret B, Varsier N, Picon O, Wiart J (2015) A new surrogate modeling technique combining Kriging and polynomial chaos expansions: application to uncertainty analysis in computational dosimetry. J Comput Phys 286:103–117
28. Khodaparast HH, Mottershead JE, Badcock KJ (2011) Interval model updating with irreducible uncertainty using the Kriging predictor. Mech Syst Signal Process 25(4):1204–1226
29. Nechak L, Gillot F, Besset S, Sinou JJ (2015) Sensitivity analysis and Kriging based models for robust stability analysis of brake systems. Mech Res Commun 69:136–145
30. Pigoli D, Menafoglio A, Secchi P (2016) Kriging prediction for manifold-valued random fields. J Multivar Anal 145:117–131
31. Wang D, DiazDelaO FA, Wang W, Lin X, Patterson EA, Mottershead JE (2016) Uncertainty quantification in DIC with Kriging regression. Opt Lasers Eng 78:182–195
32. Jeong S, Mitsuhiro M, Kazuomi Y (2005) Efficient optimization design method using Kriging model. J Aircr 42(2):413–420
33. Hanefi B, Turalioglu SF (2005) A Kriging-based approach for locating a sampling site: in the assessment of air quality. Stoch Environ Res Risk Assess 19(4):301–305
34. Den Hertog D, Kleijnen JPC, Siem AYD (2006) The correct Kriging variance estimated by bootstrapping. J Oper Res Soc 57(4):400–409
35. Xavier E (2005) Simple and ordinary multigaussian Kriging for estimating recoverable reserves. Math Geol 37(3):295–319
36. Martin JD, Simpson TW (2004) On using Kriging models as probabilistic models in design. SAE Trans J Mater Manuf 5:129–139
37. Elsayed K (2015) Optimization of the cyclone separator geometry for minimum pressure drop using Co-Kriging. Powder Technol 269:409–424
38. Thai CH, Do VNV, Nguyen-Xuan H (2016) An improved moving Kriging-based meshfree method for static, dynamic and buckling analyses of functionally graded isotropic and sandwich plates. Eng Anal Bound Elem 64:122–136
39. Yang X, Liu Y, Zhang Y, Yue Z (2015) Probability and convex set hybrid reliability analysis based on active learning Kriging model. Appl Math Model 39(14):3954–3971
40. Gaspar B, Teixeira AP, Guedes SC (2014) Assessment of the efficiency of Kriging surrogate models for structural reliability analysis. Probab Eng Mech 37:24–34
41. Huang X, Chen J, Zhu H (2016) Assessing small failure probabilities by AK–SS: an active learning method combining Kriging and subset simulation. Struct Saf 59:86–95
42. Kwon H, Choi S (2015) A trended Kriging model with R^2 indicator and application to design optimization. Aerosp Sci Technol 43:111–125
43. Sakata S, Ashida F, Zako M (2008) Kriging-based approximate stochastic homogenization analysis for composite materials. Comput Methods Appl Mech Eng 197(21–24):1953–1964
44. Luersen MA, Steeves CA, Nair PB (2015) Curved fiber paths optimization of a composite cylindrical shell via Kriging-based approach. J Compos Mater 49(29):3583–3597

45. Qatu MS, Leissa AW (1991) Natural frequencies for cantilevered doubly curved laminated composite shallow shells. Compos Struct 17:227–255
46. Qatu MS, Leissa AW (1991) Vibration studies for laminated composite twisted cantilever plates. Int J Mech Sci 33(11):927–940
47. Chakravorty D, Bandyopadhyay JN, Sinha PK (1995) Free vibration analysis of point supported laminated composite doubly curved shells: a finite element approach. Comput Struct 54(2):191–198
48. Dey S, Karmakar A (2012) Free vibration analyses of multiple delaminated angle-ply composite conical shells: a finite element approach. Compos Struct 94(7):2188–2196
49. Leissa AW, Narita Y (1984) Vibrations of corner point supported shallow shells of rectangular planform. Earthq Eng Struct Dyn 12:651–661
50. Carrera E (2003) Theories and finite elements for multilayered plates and shells: a unified compact formulation with numerical assessment and benchmarking. Arch Comput Methods Eng 10(3):215–296
51. Hu HT, Peng HW (2013) Maximization of fundamental frequency of axially compressed laminated curved panels with cutouts. Compos B Eng 47:8–25
52. Ghavanloo E, Fazelzadeh SA (2013) Free vibration analysis of orthotropic doubly curved shallow shells based on the gradient elasticity. Compos B Eng 45(1):1448–1457
53. Tornabene F, Brischetto S, Fantuzzia N, Violaa E (2015) Numerical and exact models for free vibration analysis of cylindrical and spherical shell panels. Compos B Eng 81:231–250
54. Fazzolari FA (2014) A refined dynamic stiffness element for free vibration analysis of cross-ply laminated composite cylindrical and spherical shallow shells. Compos B Eng 62:143–158
55. Mantari JL, Oktem AS, Guedes SC (2012) Bending and free vibration analysis of isotropic and multilayered plates and shells by using a new accurate higher-order shear deformation theory. Compos B Eng 43(8):3348–3360
56. Fang C, Springer GS (1993) Design of composite laminates by a Monte Carlo method. Compos Mater 27(7):721–753
57. Mahadevan S, Liu X, Xiao Q (1997) A probabilistic progressive failure model for composite laminates. J Reinf Plast Compos 16(11):1020–1038
58. Dey S, Mukhopadhyay T, Spickenheuer A, Adhikari S, Heinrich G (2016) Bottom up surrogate based approach for stochastic frequency response analysis of laminated composite plates. Compos Struct 140:712–772
59. Dey S, Mukhopadhyay T, Adhikari S (2015) Stochastic free vibration analyses of composite doubly curved shells: a Kriging model approach. Compos B Eng 70:99–112
60. Dey S, Mukhopadhyay T, Khodaparast HH, Kerfriden P, Adhikari S (2015) Rotational and ply-level uncertainty in response of composite shallow conical shells. Compos Struct 131:594–605
61. Pandit MK, Singh BN, Sheikh AH (2008) Buckling of laminated sandwich plates with soft core based on an improved higher order zigzag theory. Thin-Walled Struct 46(11):1183–1191
62. Dey S, Mukhopadhyay T, Sahu SK, Li G, Rabitz H, Adhikari S (2015) Thermal uncertainty quantification in frequency responses of laminated composite plates. Compos B Eng 80:186–197
63. Dey S, Mukhopadhyay T, Spickenheuer A, Gohs U, Adhikari S (2016) Uncertainty quantification in natural frequency of composite plates: an artificial neural network based approach. Adv Compos Lett (accepted)
64. Mukhopadhyay T, Naskar S, Dey S, Adhikari S (2016) On quantifying the effect of noise in surrogate based stochastic free vibration analysis of laminated composite shallow shells. Compos Struct 140:798–805
65. Shaw A, Sriramula S, Gosling PD, Chryssanthopoulos MK (2010) A critical reliability evaluation of fibre reinforced composite materials based on probabilistic micro and macro-mechanical analysis. Compos B Eng 41(6):446–453
66. Dey S, Mukhopadhyay T, Khodaparast HH, Adhikari S (2016) Fuzzy uncertainty propagation in composites using Gram–Schmidt polynomial chaos expansion. Appl Math Model 40(7–8):4412–4428
67. Dey S, Naskar S, Mukhopadhyay T, Gohs U, Spickenheuer A, Bittrich L, Sriramula S, Adhikari S, Heinrich G (2016) Uncertain natural frequency analysis of composite plates including effect of noise: a polynomial neural network approach. Compos Struct 143:130–142
68. Afeefa S, Abdelrahman WG, Mohammad T, Edward S (2008) Stochastic finite element analysis of the free vibration of laminated composite plates. Comput Mech 41:495–501
69. Dey S, Mukhopadhyay T, Adhikari S (2015) Stochastic free vibration analysis of angle-ply composite plates: a RS-HDMR approach. Compos Struct 122:526–553
70. Loja MAR, Barbosa JI, Mota Soares CM (2015) Dynamic behaviour of soft core sandwich beam structures using Kriging-based layerwise models. Compos Struct 134:883–894
71. Dey S, Mukhopadhyay T, Khodaparast HH, Adhikari S (2015) Stochastic natural frequency of composite conical shells. Acta Mech 226(8):2537–2553
72. Singh BN, Yadav D, Iyengar NGR (2001) Natural frequencies of composite plates with random material properties using higher-order shear deformation theory. Int J Mech Sci 43(10):2193–2214
73. Tripathi V, Singh BN, Shukla KK (2007) Free vibration of laminated composite conical shells with random material properties. Compos Struct 81(1):96–104
74. McKay MD, Beckman RJ, Conover WJ (2000) A comparison of three methods for selecting values of input variables in the analysis of output from a computer code. Technometrics 42(1):55–61
75. Bathe KJ (1990) Finite element procedures in engineering analysis. Prentice Hall Inc., New Delhi
76. Meirovitch L (1992) Dynamics and control of structures. Wiley, New York
77. Krige DG (1951) A statistical approach to some basic mine valuation problems on the witwatersrand. J Chem Metall Min Soc S Afr 52:119–139
78. Hengl T, Heuvelink GBM, Rossiter DG (2007) About regression-Kriging: from equations to case studies. Comput Geosci 33:1301–1315
79. Matías JM, González-Manteiga W (2005) Regularized Kriging as a generalization of simple, universal, and bayesian Kriging. Stoch Environ Res Risk Assess 20:243–258
80. Omre H, Halvorsen KB (1989) The Bayesian bridge between simple and universal kriging. Math Geol 21:767–786
81. Tonkin MJ, Larson SP (2002) Kriging Water Levels with a Regional-Linear and Point-Logarithmic Drift. Ground Water 40:185–193
82. Warnes JJ (1986) A sensitivity analysis for universal Kriging. Math Geol 18:653–676
83. Stein A, Corsten CA (1991) Universal Kriging and cokriging as a regression procedure on JSTOR. Biometrics 47:575–587
84. Olea RA (2011) Optimal contour mapping using Kriging. J Geophys Res 79:695–702
85. Ghiasi Y, Nafisi V (2015) The improvement of strain estimation using universal Kriging. Acta Geod Geophys 50:479–490
86. Li L, Romary T, Caers J (2015) Universal kriging with training images. Spat Stat 14:240–268
87. Joseph VR, Hung Y, Sudjianto A (2008) Blind Kriging: a new method for developing metamodels. J Mech Des 130:031102

88. Hung Y (2011) Penalized blind Kriging in computer experiments. Stat Sin 21:1171–1190
89. Couckuyt I, Forrester A, Gorissen D et al (2012) Blind Kriging: implementation and performance analysis. Adv Eng Softw 49:1–13
90. Koziel S, Bekasiewicz A, Couckuyt I, Dhaene T (2014) Efficient multi-objective simulation-driven antenna design using Co-Kriging. IEEE Trans Antennas Propag 62:5900–5905
91. Elsayed K (2015) Optimization of the cyclone separator geometry for minimum pressure drop using Co-Kriging. Powder Technol 269:409–424
92. Clemens M, Seifert J (2015) Dimension reduction for the design optimization of large scale high voltage devices using co-Kriging surrogate modeling. IEEE Trans Magn 51:1–4
93. Perdikaris P, Venturi D, Royset JO, Karniadakis GE (2015) Multi-fidelity modelling via recursive Co-Kriging and Gaussian–Markov random fields. Proc Math Phys Eng Sci 471:20150018
94. Kamiński B (2015) A method for the updating of stochastic Kriging metamodels. Eur J Oper Res 247:859–866
95. Qu H, Fu MC (2014) Gradient extrapolated stochastic Kriging. ACM Trans Model Comput Simul 24:1–25
96. Chen X, Kim K-K (2014) Stochastic Kriging with biased sample estimates. ACM Trans Model Comput Simul 24:1–23
97. Wang K, Chen X, Yang F et al (2014) A new stochastic Kriging method for modeling multi-source exposure-response data in toxicology studies. ACS Sustain Chem Eng 2:1581–1591
98. Wang B, Bai J, Gea HC (2013) Stochastic Kriging for random simulation metamodeling with finite sampling. In: 39th Design automation conference ASME, vol 3B, p V03BT03A056
99. Chen X, Ankenman BE, Nelson BL (2013) Enhancing stochastic Kriging metamodels with gradient estimators. Oper Res 61:512–528
100. Chen X, Nelson BL, Kim K-K (2012) Stochastic Kriging for conditional value-at-risk and its sensitivities. In: Proceedings of title proceedings 2012 winter simulation conference. IEEE, pp 1–12
101. Kennedy M, O'Hagan A (2000) Predicting the output from a complex computer code when fast approximations are available. Biometrika 87:1–13
102. Rivest M, Marcotte D (2012) Kriging groundwater solute concentrations using flow coordinates and nonstationary covariance functions. J Hydrol 472–473:238–253
103. Biscay Lirio R, Camejo DG, Loubes J-M, Muñiz Alvarez L (2013) Estimation of covariance functions by a fully data-driven model selection procedure and its application to Kriging spatial interpolation of real rainfall data. Stat Methods Appl 23:149–174
104. Putter H, Young GA (2001) On the effect of covariance function estimation on the accuracy of Kriging predictors. Bernoulli 7:421–438
105. Mukhopadhyay T, Chowdhury R, Chakrabarti A (2016) Structural damage identification: a random sampling-high dimensional model representation approach. Adv Struct Eng. doi:10.1177/1369433216630370
106. Mukhopadhyay T, Dey TK, Chowdhury R, Chakrabarti A (2015) Structural damage identification using response surface based multi-objective optimization: a comparative study. Arabian J Sci Eng 40(4):1027–1044